Jigsaw Game: Federated Clustering

Anonymous authors
Paper under double-blind review

Abstract

Federated learning has recently garnered significant attention, especially within the domain of supervised learning. However, despite the abundance of unlabeled data on end-users, unsupervised learning problems such as clustering in the federated setting remain underexplored. In this paper, we investigate the federated clustering problem, with a focus on federated k-means. We outline the challenge posed by its non-convex objective and data heterogeneity in the federated framework. To tackle these challenges, we adopt a new perspective by studying the structures of local solutions in k-means and propose a one-shot algorithm called FeCA (Federated Centroid Aggregation). FeCA adaptively refines local solutions on clients, then aggregates these refined client solutions to recover the global solution of the entire dataset in a single round. We empirically demonstrate the robustness of FeCA under various federated scenarios on both synthetic and real-world data. Additionally, we extend FeCA to representation learning and present DeepFeCA, which combines DeepCluster and FeCA for unsupervised feature learning in the federated setting.

1 Introduction

Federated learning (FL) has emerged as a promising framework, enabling model training across decentralized data. This approach addresses data privacy concerns by allowing data to remain on individual clients. The goal of FL is to collaboratively train a model across multiple clients without directly sharing data. Within this context, FedAvg McMahan et al. (2017) has been considered the standard approach in FL, designed to obtain a centralized model by averaging the models trained independently on each client's data.

Although FL has seen widespread applications in the domain of supervised learning, particularly in tasks like classification (Oh et al., 2021; Jiménez-Sánchez et al., 2023), its utilization in the unsupervised learning sphere is still largely unexplored, even though it holds significant potential and applicability in numerous practical situations. A notable example is the large collections of unlabeled photographs owned by most smartphone users. In such instances, federated unsupervised learning emerges as a potent paradigm, allowing unsupervised learning approaches to harness the "collective wisdom" inherent in these unlabeled data, all while safeguarding user privacy.

In this paper, we investigate federated unsupervised learning, particularly focusing on the popular clustering problem of k-means. In prior studies, clustering methods have been applied in FL mainly focusing on problems, such as client selection (Ghosh et al., 2020; Long et al., 2023) and privacy enhancement (Li et al., 2022; Elhussein & Gürsoy, 2023), without a deep investigation into the unsupervised learning aspect. Moreover, existing distributed clustering methods overlook the unique challenges in FL, such as data heterogeneity and communication efficiency, making it difficult to apply in the federated setting. Our study extends to federated clustering, ~~aiming to incorporate~~ incorporating unsupervised clustering on individual clients within a federated framework.

One key challenge of federated clustering is the inherent non-convex nature of clustering problems, presenting multiple equivalent global solutions and potentially even more local solutions. Standard algorithms like Lloyd's algorithm Lloyd (1982) can only find a local solution of the k-means problem, without guaranteeing global optimum. *We note that the term "local solution" in this context refers to a local optimal in optimiza-*

tion, not the solution learned from a client[1]. This challenge is amplified in the federated setting, where each client's data is a distinct subset of the entire dataset. Even under the IID data split condition, each client's clustering results might be a suboptimal local solution. Such solutions contain spurious centroids that are far from true centroids of the global solution. These spurious centroids make it more challenging for the central server to accurately recover the true centroids of the entire dataset in the federated setting. And this issue could become even more pronounced under non-IID conditions.

To this end, we propose a novel one-shot federated k-means algorithm: Federated Centroid Aggregation (FeCA), offering a new perspective of exploiting structured local solutions. In the k-means problem, local solutions carry valuable information from the global solution. The proposed algorithm resolves these local solutions and leverages their benign properties within the federated clustering framework. FeCA is built upon theoretical studies (Qian et al., 2021; Chen & Xi, 2020) presented in centralized k-means, that demonstrate every local solution is structured and contains nontrivial information about the global solution. Specifically, some spurious centroids from local solutions, whose clusters include data from a single true cluster, can be merged to approximate one true centroid. Other spurious centroids, whose clusters contain data from multiple true clusters, can be ignored since it is located far from any true centroid. These local solution structures can be utilized in the federated setting as well.

One common concern of FL lies in the potential decrease in performance compared to centralized models, because of the data heterogeneity across clients. However, from the local solution point of view, federated clustering could benefit from this decentralized framework. Each client's solution, whether a local optimum or not, carries partial information about the global solution of the entire dataset. By incorporating multiple clients' solutions, the central server could potentially recover the global optimal solution in one shot, akin to assembling a *jigsaw* puzzle of clients' solutions. For example, a true centroid missing from one client's solution could be identified by other clients' solutions.

Therefore, FeCA is designed to recover the global solution for k-means clustering in a federated setting by refining and extracting partial solutions from clients, and then aggregating them on the server. First, Lloyd's algorithm for k-means is performed on each client's data. Then, FeCA leverages structural properties to adaptively refine spurious centroids and obtain a set of refined centroids for each client. These sets of refined centroids are then sent to the server, where FeCA aggregates them to recover the global solution of the entire dataset. By exploiting structured local solutions, FeCA is able to accurately identify the true k centroids of the entire dataset in a one-shot federated setting.

We further extend FeCA beyond a pre-defined feature space to the modern deep feature framework (Liu et al., 2021). We present DeepFeCA, a federated representation learning algorithm from decentralized unlabeled data. Concretely, we pair FeCA with clustering-based deep representation learning models such as DeepCluster Caron et al. (2018; 2020), which assigns pseudo-labels according to k-means clustering and then learns the neural network in a supervised fashion. The resulting algorithm iterates between applying FeCA on the current features and DeepCluster.

We evaluate both FeCA and DeepFeCA on benchmark datasets, including S-sets Fränti & Sieranoja (2018), CIFAR Krizhevsky et al. (2009), and Tiny-ImageNet Le & Yang (2015). FeCA consistently outperforms baselines in various federated settings, showing its effectiveness in recovering the global solution. And DeepFeCA shows promising performance in federated representation learning.

2 Related Work

Federated learning. Mainstream FL algorithms (McMahan et al., 2017; Khaled et al., 2020; Haddadpour & Mahdavi, 2019) adopt coordinate-wise averaging of the weights from clients. However, given the limited performance of direct averaging, other approaches have been proposed: Yurochkin et al. (2019); Wang et al. (2020); Zhang et al. (2023b); Tan et al. (2023) identify the permutation symmetry in neural networks and then aggregate after the adaptive permutation; Lin et al. (2020); He et al. (2020); Zhou et al. (2020); Chen

[1]For clarity, throughout this paper, we use the client's solution for the result obtained from a client. If the solution happens to be a local solution, we name it the client's local solution.

& Chao (2021); Zeng et al. (2023) replace weight average by model ensemble and distillation. These studies enhance the performance of the synchronization scheme but overlook the impact of local solutions on clients.

Federated Clustering. Many distributed clustering methods (Balcan et al., 2013; Bachem et al., 2018; Kargupta et al., 2001; Januzaj et al., 2004; Hess et al., 2022) have been proposed, but they overlook the heterogeneous challenge in FL. For synchronizing results returned from different clustering solutions, consensus clustering has been studied widely (Monti et al., 2003; Goder & Filkov, 2008; Li et al., 2021). But it works on the same dataset, unlike FL. In the context of FL, Qiao et al. (2021); Li et al. (2023); Xia et al. (2020); Lu et al. (2023); Li et al. (2022) focus on communication efficiency or privacy-preserving. A recent federated clustering study Stallmann & Wilbik (2022) proposes weighted averaging for Fuzzy c-means but requires multiple rounds. The study most relevant to ours introduces k-FED Dennis et al. (2021), a one-shot federated clustering algorithm, under a rather strong assumption that each client only has data from a few true clusters. It is still underexplored for federated clustering and usage of local solutions.

Federated representation learning. FedRep Collins et al. (2021) studies supervised representation learning by alternating updates between classifiers and feature extractors. Jeong et al. (2020); Zhang et al. (2020) study federated semi-supervised learning with the server holding some labeled data and clients having unlabeled data. For federated unsupervised learning, Zhuang et al. (2021) proposes self-supervised learning in non-IID settings with a divergence-aware update strategy for mitigating non-IID challenges, distinct from our clustering focus. Zhang et al. (2023a) adopts the contrastive approach for model training on clients. A recent framework Lubana et al. (2022) introduces federated unsupervised learning with constrained clustering for representation learning, while our focus lies on exploring federated clustering via local solutions.

3 Background

Clustering. Given a d-dimensional dataset $\mathcal{D} = \{x_1 \in \mathbb{R}^d, \ldots, x_N \in \mathbb{R}^d\}$, the goal of k-means problem is to identify a set of k centroids $\mathcal{C} = \{c_1 \in \mathbb{R}^d, \ldots, c_k \in \mathbb{R}^d\}$ that minimize the following objective

$$G(\mathcal{C}) \doteq \sum_{n=1}^{N} \min_{j \in [k]} \|x_n - c_j\|_2^2. \tag{1}$$

Federated clustering. In the federated setting, the dataset $\mathcal{D}$ is decentralized across M clients. Each client $m \in [M]$ possesses a distinct subset $\mathcal{D}_m$ of the entire dataset $\mathcal{D}$. Despite different data configurations, the goal of federated clustering remains the same – to identify k centroids $\mathcal{C} = \{c_1, \ldots, c_k\}$ for $\mathcal{D} = \cup_m \mathcal{D}_m$. Under this federated framework, the optimization problem in Equation 1 can be reformulated as

$$\min_{\mathcal{C}} \; G(\mathcal{C}) = \sum_{m=1}^{M} \frac{|\mathcal{D}_m|}{|\mathcal{D}|} G_m(\mathcal{C}), \tag{2}$$

where G_m is the k-means objective computed on $\mathcal{D}_m$. Due to privacy concerns that restrict direct data sharing among clients, the optimization problem described in Equation 2 cannot be solved directly. Thus, the proposed algorithm FeCA utilizes a collaborative approach between clients and a central server. Initially, each client independently minimizes $G_m(\mathcal{C})$ to obtain k centroids $\mathcal{C}^{(m)} = \{c_1^{(m)}, \ldots, c_k^{(m)}\}$ from their dataset $\mathcal{D}_m$. Then the server aggregates centroids $\cup_m \mathcal{C}^{(m)}$ to find a set of k centroids $\mathcal{C}$ for $\mathcal{D}$.

We note that when clients perform standard Lloyd's algorithm for k-means clustering, they usually end up with local solutions of $\min_{\mathcal{C}} G_m(\mathcal{C})$, resulting in suboptimal performance even with IID distributed data $\mathcal{D}_m$. These local solutions can significantly complicate the aggregation process on the server. Thus, one key challenge in federated clustering lies in effectively resolving client's local solutions and appropriately aggregating them on the central server.

3.1 Structure of Local Solutions

To better resolve the federated clustering problem, we propose to take a deeper look at local solutions in k-means, which often significantly differ from the global minimizer. Recent theoretical works by Qian et al.

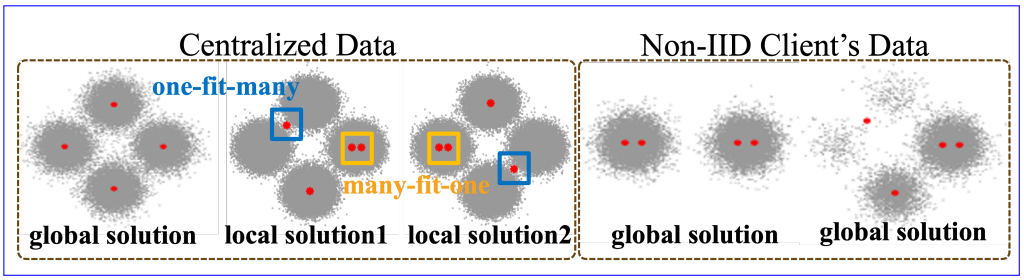

Figure 1: **Clustering results.** (Left): global and local solutions on centralized/IID client's data; (Right): global solutions for non-IID client's data sharing similar structures.

(2021); Chen & Xi (2020) have established a positive result that under certain separation conditions, all the local solutions share a common geometric structure. More formally, ~~consider~~ suppose a local solution ~~that~~ identifies centroids $\{c_1, \ldots, c_k\}$~~, then~~. Then, there exists a one-to-one ~~mapping between centroids $\{c_1, \ldots, c_k\}$~~ association between these centroids and the true centers $\{c_1^*, \ldots, c_k^*\}$~~such~~. This association ensures that each centroid c_i must belong to exactly one of the following cases with overwhelming probability[2]:

- **Case 1** (one-fit-many association): centroid c_i is ~~mapped to~~ associated with s $(s > 1)$ true centers $\{c_{j_1}^*, \ldots, c_{j_s}^*\}$~~;~~.
- **Case 2** (one/many-fit-one association): t $(t \geq 1)$ centroids $\{c_{i_1}, \ldots, c_{i_t}\}$ are all ~~mapped to~~ associated with one true center c_j^*.

Namely, a centroid c_i in a local solution is either a *one-fit-many* centroid that is located in the middle of multiple true centers (case 1, when $s > 1$), or a *one/many-fit-one* centroid that is close to a true center (case 2). Notably, when c_i is the only centroid near a true center (case 2, when $t = 1$), it is considered a correctly identified centroid that closely approximates a true center. An illustration is provided in Figure 1, which also shows that similar structures emerge even with non-IID distributed data. Next, we will introduce how our algorithm utilizes such local solution structures to obtain unified clustering results in the federated setting.

4 Jigsaw Game – FeCA

The proposed federated clustering algorithm FeCA is built upon the collaboration between clients and a central server. Each client m shares its refined centroid solution $\mathcal{C}^{(m)}$ with the server, where every $\mathcal{C}^{(m)}$ carries partial information of the global solution, much like pieces of a jigsaw puzzle. Then the server aggregates received centroids $\cup_m \mathcal{C}^{(m)}$ to obtain a unified complete solution $\mathcal{C}^*$, akin to assembling puzzle pieces in a *jigsaw game*. FeCA only requires one communication between clients and the server, thanks to its adaptive refinement of local solutions on the client side. The detailed procedure is presented in Algorithm 1 and shown in Figure 2.

Algorithm 1 Federated Centroid Aggregation (FeCA)

input cluster number k
for each client $m = 1, \ldots, M$ **do**
  $\mathcal{C}^{(m)}, \mathcal{D}^{(m)} \leftarrow$ ClientUpdate (k)
  $\mathcal{R}^{(m)} \leftarrow$ RadiusAssign $(\mathcal{C}^{(m)}, \mathcal{D}^{(m)})$
end for
$\mathcal{C} \leftarrow \bigcup_{m=1}^{M} \mathcal{C}^{(m)}$
$\mathcal{R} \leftarrow \bigcup_{m=1}^{M} \mathcal{R}^{(m)}$
$\mathcal{C}^* \leftarrow$ ServerAggregation $(k, \mathcal{C}, \mathcal{R})$
return $\mathcal{C}^*$

[2]Such structure of local solutions holds even when $k \neq k^*$, where k^* is the number of true clusters in the dataset.

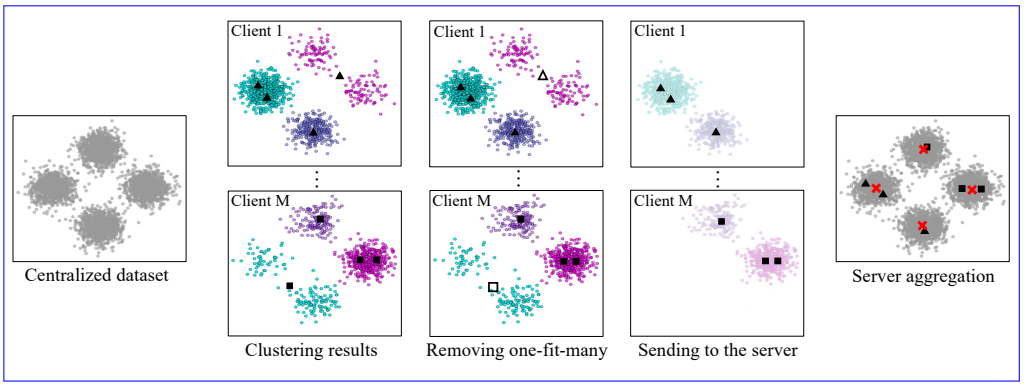

Figure 2: **FeCAroadmap.** 1st column: The centralized dataset distributed to clients. 2nd column: K-means clustering results on different clients under non-IID data split condition, where black triangles and squares represent centroids. 3rd column: Eliminating one-fit-many centroids in Algorithm 2, indicated by hollow squares and triangles. 4th column: Centroids sent to the server. 5th column: Aggregation of received centroids on the server where red crosses represent recovered centroids.

Privacy concern. While privacy is crucial in FL, it is not our main focus. However, an advantage of our one-shot algorithm is its minimal information exchange compared to standard iterative approaches like distributed clustering. Sending refined centroids to the server in FeCA is viewed as no more privacy risk than mainstream FL approaches of sending models with classifiers, which more or less convey class or cluster information.

4.1 Client Update Algorithm

Algorithm 2 FeCA- ClientUpdate

input cluster number k
Apply Lloyd's algorithm on the data of client m to obtain k clusters $\mathcal{D}^{(m)} = \{\mathcal{D}_1^{(m)}, \ldots, \mathcal{D}_k^{(m)}\}$ and k centroids $\mathcal{C}^{(m)} = \{c_1^{(m)}, \ldots, c_k^{(m)}\}$.
while $\mathcal{C}^{(m)} \neq \oslash$ **do**
  Detect one-fit-many centroid $c_i^{(m)}$ whose cluster $\mathcal{D}_i^{(m)}$ has the largest standard deviation and calculate the objective value $G_i^{(m)}$ of the cluster $\mathcal{D}_i^{(m)}$.
  Detect many-fit-one centroids $c_p^{(m)}$, $c_q^{(m)}$ of clusters $\mathcal{D}_p^{(m)}$ and $\mathcal{D}_q^{(m)}$ with the smallest pairwise distance.
  Merge $\mathcal{D}_p^{(m)}$ and $\mathcal{D}_q^{(m)}$ into one cluster $\mathcal{D}_j^{(m)}$ to obtain a new centroid $c_j^{(m)}$ and calculate the objective value $G_j^{(m)}$ of the merged cluster $\mathcal{D}_j^{(m)}$.
  if $G_i^{(m)} \geq G_j^{(m)}$ **then**
    $\mathcal{C}^{(m)} \leftarrow \mathcal{C}^{(m)} \setminus \{c_i^{(m)}\}$
    $\mathcal{D}^{(m)} \leftarrow \mathcal{D}^{(m)} \setminus \{\mathcal{D}_i^{(m)}\}$
  else
    Terminate the loop.
  end if
end while
return centroids $\mathcal{C}^{(m)}$, clusters $\mathcal{D}^{(m)}$

This step aims to refine the spurious local solutions of k-means clustering on clients. Each client m first performs standard Lloyd's algorithm to obtain a set of k centroids $\mathcal{C}^{(m)} = \{c_1^{(m)}, \ldots, c_k^{(m)}\}$, and this solution is only guaranteed to be a local solution. As discussed in subsection 3.1, despite the variations in solutions across different clients, each $\mathcal{C}^{(m)}$ always possesses some centroids (one/many-fit-one) that are proximate to

a subset of ground truth centers. To facilitate the aggregation process on the server, we propose retaining only centroids from $\mathcal{C}^{(m)}$ that are positioned close to true centers.

The client update step in FeCA focuses on refining the solution $\mathcal{C}^{(m)}$ by eliminating one-fit-many centroids that are distant from any true center. Specifically, a one-fit-many centroid is always located in the middle of multiple nearby true clusters, making it distant from most data points in those clusters and leading to a high standard deviation for its cluster. Conversely, many-fit-one centroids, which fit the same true center, are close to each other and thus have a small pairwise distance. As presented in Algorithm 2, we first use these properties to detect the candidate one-fit-many $c_i^{(m)}$ and many-fit-one $c_p^{(m)}, c_q^{(m)}$ centroids, which are likely from a spurious local solution.

Next, for further refinement, we need to confirm if these candidate centroids indeed originate from a local solution. To this end, for detected one-fit-many centroid $c_i^{(m)}$, we first calculate the objective value $G_i^{(m)}$ of its cluster $\mathcal{D}_i^{(m)}$ as

$$G_i^{(m)} = \sum\nolimits_{x \in \mathcal{D}_i^{(m)}} \|x - c_i^{(m)}\|_2^2. \tag{3}$$

For detected many-fit-one centroids, we merge their clusters $\mathcal{D}_p^{(m)}, \mathcal{D}_q^{(m)}$ to form a new cluster $\mathcal{D}_j^{(m)}$ with centroid $c_j^{(m)}$. And then we calculate the objective value $G_j^{(m)}$ as

$$G_j^{(m)} = \sum\nolimits_{x \in \{\mathcal{D}_p^{(m)} \cup \mathcal{D}_q^{(m)}\}} \|x - c_j^{(m)}\|_2^2. \tag{4}$$

If the current solution $\mathcal{C}^{(m)}$ is only locally optimal, $\mathcal{D}_i^{(m)}$ should contain data from multiple true clusters with a large $G_i^{(m)}$, while $\mathcal{D}_j^{(m)}$ only contains data from one true cluster with a small $G_j^{(m)}$. Therefore, if $G_i^{(m)}$ is greater than $G_j^{(m)}$, it confirms that these candidate centroids stem from a local solution. In such cases, Algorithm 2 removes $c_i^{(m)}$ from $\mathcal{C}^{(m)}$ for not being close to any true center. Otherwise, if $G_i^{(m)}$ is less than $G_j^{(m)}$, these centroids are regarded as the correct portion with no need for further refinement.

Notably, there may be multiple groups of centroids that possess the local structure. The algorithm is designed to iteratively identify and refine the local solution. Our theoretical analysis (Lemma A.1 in the appendix) demonstrates that Algorithm 2 effectively removes all one-fit-many centroids from local solutions under the Stochastic Ball Model.

4.2 Radius Assign Algorithm

After removing one-fit-many centroids in the ClientUpdate phase, only centroids near true centers (one/many-fit-one) would be sent to the server. This RadiusAssign step prepares these centroids for server-side aggregation by assigning a specific radius to each. This setup allows the server to utilize these radii for effective aggregation. The primary goal of this step is to determine the radius that best approximates the true cluster radius of the entire dataset. In this section, we present two algorithmic variants for the RadiusAssign step. The first variant Algorithm 3 is designed for *theoretical* validation purposes, while the second variant Algorithm 4 is tailored for *empirical* experimentation.

Through the theoretical variant, we establish Theorem 4.1 that characterizes the performance of our ~~proposed~~ algorithm FeCA under the Stochastic Ball Model. This theoretical variant generates a tentative solution $\tilde{\mathcal{C}}^{(m)}$ by discarding any potential many-fit-one centroids within $\mathcal{C}^{(m)}$. We note that the method for ~~distinguishing~~ identifying many-fit-one ~~and one-fit-one~~ centroids utilized in this theoretical variant is only applicable under the Stochastic Ball Model. Following this, a radius $r^{(m)}$ is then calculated according to the minimum pairwise distance among centroids in $\tilde{\mathcal{C}}^{(m)}$, and this radius is assigned to every centroid in the original solution $\mathcal{C}^{(m)}$ from ~~the ClientUpdate step~~Algorithm 2.

However, in real-world applications, especially under non-IID conditions, it is both challenging and unnecessary to eliminate all many-fit-one centroids, as they often align closely with true centers. Accordingly, we develop an empirical variant, Algorithm 4, which assumes only one-fit-many centroids are excluded and assigns a unique radius $r_i^{(m)}$ to each centroid $c_i^{(m)} \in \mathcal{C}^{(m)}$. As for remaining many-fit-one centroids, their

Algorithm 3 FeCA- RadiusAssign (*Theoretical*)

input centroids $\mathcal{C}^{(m)}$, clusters $\mathcal{D}^{(m)}$
Initialize a new set of centroids $\tilde{\mathcal{C}}^{(m)} = \mathcal{C}^{(m)}$.
Determine r'_i for each centroid $\tilde{c}_i^{(m)} \in \tilde{\mathcal{C}}^{(m)}$ as the maximum distance from any data point in $\mathcal{D}_i^{(m)}$ to $\tilde{c}_i^{(m)}$: $r'_i = \max_{x_i^{(m)} \in \mathcal{D}_i^{(m)}} \|x_i^{(m)} - \tilde{c}_i^{(m)}\|_2$.
for each centroid $\tilde{c}_i^{(m)} \in \tilde{\mathcal{C}}^{(m)}$ **do**
  Identify the nearest centroid $\tilde{c}_{j\neq i}^{(m)} \in \tilde{\mathcal{C}}^{(m)}$ to $\tilde{c}_i^{(m)}$ with the pairwise distance denoted as d_{ij}.
  if $r'_i + r'_j > d_{ij}$ **then**
    $\tilde{\mathcal{C}}^{(m)} \leftarrow \tilde{\mathcal{C}}^{(m)} \setminus \{\tilde{c}_i^{(m)}, \tilde{c}_j^{(m)}\}$
  end if
end for
Calculate the minimal pairwise distance $\tilde{\Delta}_{min}^{(m)}$ between centroids in $\tilde{\mathcal{C}}^{(m)}$: $\tilde{\Delta}_{min}^{(m)} = \min_{\tilde{c}_i, \tilde{c}_j \in \tilde{\mathcal{C}}^{(m)}, i\neq j} \|\tilde{c}_i - \tilde{c}_j\|_2$.
Determine the uniform radius $r^{(m)} = \frac{1}{2}\tilde{\Delta}_{min}^{(m)}$ which is assigned to each centroid in $\mathcal{C}^{(m)}$.
$\mathcal{R}^{(m)} \leftarrow \bigcup_i \left(c_i^{(m)}, r^{(m)}\right)$
return $\mathcal{R}^{(m)}$

Algorithm 4 FeCA- RadiusAssign (*Empirical*)

input centroids $\mathcal{C}^{(m)}$, clusters $\mathcal{D}^{(m)}$
Determine r'_i for each centroid $c_i^{(m)} \in \mathcal{C}^{(m)}$ as the maximum distance from any data point in $\mathcal{D}_i^{(m)}$ to $c_i^{(m)}$: $r'_i = \max_{x_i^{(m)} \in \mathcal{D}_i^{(m)}} \|x_i^{(m)} - c_i^{(m)}\|_2$.
for each centroid $c_i^{(m)} \in \mathcal{C}^{(m)}$ **do**
  Identify the nearest centroid $c_{j\neq i}^{(m)} \in \mathcal{C}^{(m)}$ to $c_i^{(m)}$ with the pairwise distance denoted as d_{ij}, and then calculate $r''_i = \frac{1}{2}d_{ij}$.
  Determine the unique radius $r_i^{(m)} = \min(r'_i, r''_i)$ which is assigned to the centroid $c_i^{(m)}$.
end for
$\mathcal{R}^{(m)} \leftarrow \bigcup_i \left(c_i^{(m)}, r_i^{(m)}\right)$
return $\mathcal{R}^{(m)}$

radii are estimated as half of their pairwise distances, which are typically much smaller compared to those of correct centroids. The server then groups all received centroids based on these radii, prioritizing the largest ones first. This ensures that the smaller radii associated with many-fit-one centroids minimally impact the aggregation process. An in-depth analysis of Algorithm 4 is provided in Appendix B, showcasing its effectiveness across a variety of experimental settings, including those with high data heterogeneity.

It is worth noting that the theoretical variant is designed for theoretical analysis under the Stochastic Ball Model assumption. This assumption enables easy identification of many-fit-one centroids for clearer cluster separation approximation and radius assignment. In contrast, the empirical variant does not need to remove many-fit-one centroids, as they are close to true centers and aid in global solution reconstruction on the server side. This approach allows the empirical variant to assign distinct radii to each remaining centroid, enhancing the algorithm's effectiveness and practicality without relying on limited assumptions. A detailed comparison is provided in subsection C.4.

4.3 Server Aggregation Algorithm

At the server stage, the goal is to aggregate all received centroids $\mathcal{C} = \{\mathcal{C}^{(1)}, \ldots, \mathcal{C}^{(M)}\}$ from M clients into a unified set of k centroids $\mathcal{C}^*$. This task presents apparent challenges: due to the preceding refinement stage, clients may contribute varying numbers of centroids, and the indices of these centroids often lack consistency across clients. However, assuming the refinement phase in Algorithm 2 effectively removes spurious one-

Algorithm 5 FeCA- ServerAggregation

input cluster number k, centroids $\mathcal{C}$, radius $\mathcal{R}$
$n = 1$
while $\mathcal{C} \neq \oslash$ **do**
  Pick $(c_i, r_i) \in \mathcal{R}$ with the largest r_i.
  Let $\mathcal{S}_n = \{c_t : c_t \in \mathcal{C}, \|c_t - c_i\|_2 \leq r_i\}$
  Set $\mathcal{C} \leftarrow \mathcal{C} \setminus \mathcal{S}_n$
  $n = n + 1$
end while
Select top k sets $\mathcal{S}_n$ containing the largest number of elements.
$\mathcal{C}^* \leftarrow \text{mean}(\mathcal{S}_j), j \in [k]$
return $\mathcal{C}^*$

fit-many centroids far from true centers, the returned centroids on the server would be closely grouped around true centers. This phenomenon enables a straightforward classification of all returned centroids into k distinct groups, each aligned with one of the k true centers, as presented in Algorithm 5. Equivalently, this is another clustering problem based on returned centroids under a high Signal-to-Noise Ratio (SNR) separation condition. Finally, the server calculates the means of centroids within each group to obtain $\mathcal{C}^*$.

In some extreme cases where the number of groups n might be less than k, such as when all clients converge to the same local solution. In such cases, Algorithm 2 removes one-fit-many centroids associated with the same true clusters from all clients. This renders it impossible for Algorithm 5 to reconstruct corresponding centers without receiving any associated centroids from clients. It is important to note that this scenario is trivial within the federated framework, where all clients share the same local solutions. Essentially, it is akin to having only one client encountering a local solution. Further discussion on cases when $n < k$ is provided in the Appendix E.

4.4 Theoretical Anlysis

We now state our main theorem, which characterizes the performance of FeCA under the Stochastic Ball Model. Assume the data $x^{(m)}$ of client m is sampled independently and uniformly from one of k disjoint balls $\mathbb{B}_s$ with radius r, each centered at a true center θ_s^*, $s \in [k]$. Each ball component under the Stochastic Ball Model has a density

$$f_s(x) = \frac{1}{\text{Vol}(\mathbb{B}_s)} \mathbb{1}_{\mathbb{B}_s}(x). \tag{5}$$

Additionally, we define the maximum and minimum pairwise separations between the true centers $\{\theta_s^*\}_{s\in[k]}$ as

$$\Delta_{max} := \max_{s \neq s'} \|\theta_s^* - \theta_{s'}^*\|_2, \quad \Delta_{min} := \min_{s \neq s'} \|\theta_s^* - \theta_{s'}^*\|_2.$$

Theorem 4.1. *(Main theorem) Under the Stochastic Ball Model, for some constants $\lambda \geq 3$ and $\eta \geq 5$, if*

$$\Delta_{max} \geq 4\lambda^2 k^4 r \quad \textit{and} \quad \Delta_{min} \geq 10\eta\lambda k^2 \sqrt{r\Delta_{max}},$$

then by utilizing the radius determined by Algorithm 3 (Theoretical), for output centroids $\mathcal{C}^* = \{c_1^*, \ldots, c_k^*\}$ from Algorithm 1, the following holds:

$$\|c_s^* - \theta_s^*\|_2 \leq \frac{4}{5\eta} \Delta_{min}, \quad \forall s \in [k]. \tag{6}$$

Theorem 4.1 characterizes the performance of our main algorithm FeCA, utilizing the radius from the theoretical variant (Algorithm 3) under a homogeneous setting and high SNR condition. However, such

conditions are often not met in practical applications. Thus, we develop the empirical variant, Algorithm 4, that does not require the elimination of many-fit-one centroids and assigns a unique radius to each returned centroid from the client. A detailed analysis of these unique radii determined by Algorithm 3 (empirical) is presented in Appendix B, showcasing their effectiveness in supporting the main algorithm FeCA.

4.5 Dealing with Data Heterogeneity

So far we assume that the client's local solution for its dataset $\mathcal{D}_m$ is also a local solution of the entire dataset $\mathcal{D} = \cup_m \mathcal{D}_m$, which allows us to leverage the structures discussed in subsection 3.1. This assumption holds when $\mathcal{D}_m$ is an IID-sampled subset from $\mathcal{D}$. However, our experiments showcase our algorithm's robustness even under non-IID conditions. Here we provide an explanation in Figure 1, where right plots illustrate two clients' non-IID sampled data and the corresponding *global* solutions (achieve a global optimum when $k = k^*$[3]). We found that despite the data heterogeneity, the clients' global solutions share similar structures as described in subsection 3.1. We attribute these observations to the fact that under non-IID conditions, clients' data tend to concentrate on some of the true clusters. This increases the chance that clients' global solutions contain many-fit-one centroids for those true clusters, which can be aggregated together on the server by our algorithm FeCA. This scenario also suggests that even if a client can recover the global solution on its non-IID data, such a global solution coincides with a local solution on IID data and we still need to deploy FeCA to produce the final solution.

5 DeepFeCA

Algorithm 6 DeepFeCA for Representation Learning

Input: cluster number k, total number of clients M, round number T
Initialization: server model $\bar{\boldsymbol{\theta}}$
for round $t = 1, \cdots, T$ **do**
  Perform FeCA with M clients to obtain k aggregated centroids $\mathcal{C}^*$ (k-means clustering is performed on features extracted by $f_{\bar{\boldsymbol{\theta}}}$ on each client).
  Broadcast $\bar{\boldsymbol{\theta}}$ and $\mathcal{C}^*$ to all clients.
  for each client $m \in [M]$ **do**
    Create $\mathcal{D}_m = \{(x_n^{(m)}, \hat{y}_n^{(m)})\}_{n=1}^{N_m}$ where $\hat{y}_n^{(m)} = \arg\min_j \|x_n^{(m)} - c_j\|_2$ and $c_j \in \mathcal{C}^*$.
    Train $\bar{\boldsymbol{\theta}}$ together with a linear classifier on $\mathcal{D}_m$ for multiple epochs to obtain the client model $\boldsymbol{\theta}^{(m)}$.
  end for
  $\bar{\boldsymbol{\theta}} \leftarrow \sum_{m=1}^{M} \frac{|\mathcal{D}_m|}{|\mathcal{D}|} \boldsymbol{\theta}^{(m)}$
end for
Return the model $\bar{\boldsymbol{\theta}}$

With FeCA, we can learn centroids $\mathcal{C}^*$ in the pre-defined feature space collaboratively with multiple clients. In this section, we extend FeCA to unsupervised representation learning Liu et al. (2021), aiming to learn a feature extractor $f_{\boldsymbol{\theta}}$ parameterized by $\boldsymbol{\theta}$ from the unlabeled data set $\mathcal{D}$, such that the extracted feature $f_{\boldsymbol{\theta}}(x)$ of data x can better characterize its similarity or dissimilarity to other data instances.

Some studies (Asano et al., 2020; Caron et al., 2020; 2018) integrate clustering approaches with unsupervised representation learning. For instance, Caron et al. (2018) proposed DeepCluster, which learns $f_{\boldsymbol{\theta}}(x)$ from an unlabeled dataset $\mathcal{D} = \{x_n\}_{n=1}^N$ by repeating two steps:

- Perform Lloyd's algorithm on $\{f_{\boldsymbol{\theta}}(x_n)\}_{n=1}^N$ to obtain a set of k centroids $\mathcal{C} = \{c_j\}_{j=1}^k$;
- Create a pseudo-labeled set $\mathcal{D} = \{(x_n, \hat{y}_n)\}_{n=1}^N$ where $\hat{y}_n = \arg\min_j \|x_n - c_j\|_2$, and learn $f_{\boldsymbol{\theta}}$ with a linear classifier in a supervised fashion for multiple epochs.

DeepCluster is known for its simplicity and has been shown to perform on par with other more advanced self-supervised learning methods for representation learning Ericsson et al. (2021). In this paper, we extend

[3] k^* indicates the number of true centers in the entire dataset.

DeepCluster to the federated setting and propose DeepFeCA, which integrates DeepCluster within the FedAvg McMahan et al. (2017) framework. Namely, DeepFeCA iterates between local training of $f_{\boldsymbol{\theta}}(x)$ on each client and global model aggregation for multiple rounds. At the end of each round, DeepFeCA applies FeCA to update the centroids that are used to assign pseudo labels. Algorithm 6 outlines our approach, where the red text corresponds to FeCA, the blue text corresponds to DeepCluster, and the green text corresponds to the element-wise weight average of FedAvg.

6 Experiments

We first evaluate FeCA on benchmark synthetic datasets, which have well-established true centers. Then we extend our evaluation to frozen features of real-world image data extracted from pre-trained neural networks. Additionally, we assess the representation learning capabilities of DeepFeCA by training a deep feature extractor network from scratch in the federated framework.

To simulate the non-IID data partitions, we follow Hsu et al. (2019) to split the data drawn from Dirichlet(α) for multiple clients. Smaller α indicates that the split is more heterogeneous. We also include the IID setting, in which clients are provided with uniformly split subsets of the entire dataset. Furthermore, we have standardized the number of clients to $M = 10$ for all experiments in this section. A detailed discussion on the impact of varying the number of clients is provided in Appendix D.

Baselines. We mainly compare three baselines:

- **Match Averaging (M-Avg)**: an intuitive method without considering local solutions. M-Avg matches different sets of centroids from clients by minimizing their ℓ_2 distances and returns the means of matched centroids.
- **k-FED**: the one-shot federated clustering method Dennis et al. (2021) designed for heterogeneous data, assuming that each client's data originates from $k' \leq \sqrt{k^*}$ true clusters. The method utilizes this small k' for k-means clustering on clients. In the following experiments, we select unique k' for each dataset, with detailed tuning experiments provided in subsection C.5.
- **FFCM**: the federated clustering method proposed in Stallmann & Wilbik (2022). FFCM focuses on fuzzy c-means clustering and presents two versions of aggregation algorithms, which are weighted averaging centroids (v1) and applying k-means on centroids (v2). Since this method is not designed in one shot, we report its results for both round 1 and round 10 in the following experiments.

Additionally, we include a **Centralized** benchmark, representing the performance of k-means clustering on the entire dataset without federated splits. In the following experiments, we set $k = k^*$ for all methods except for k-FED.

Evaluation metric. For synthetic datasets with known true centers, we assess recovered centroids by calculating the ℓ_2-distance between returned centroids and true centers. In contrast, for real datasets where true centers are unknown, we evaluate clustering assignments generated from recovered centroids. We adopt the standard clustering measures including *Purity* and *Normalized Mutual Information (NMI)*. The average Purity among all clusters is reported. And NMI measures the mutual information shared between clustering assignments X and true labels Y defined as $NMI(X, Y) = 2I(X; Y)/(H(X) + H(Y))$, where I denotes the mutual information and H is the entropy.

6.1 FeCA Evaluation

On synthetic datasets. We evaluate our algorithm FeCA on benchmark datasets in Fränti & Sieranoja (2018) with known true centers. Specifically, we focus on S-sets, comprising synthetic data characterized by four different degrees of separation. S-sets includes four sets: S1, S2, S3, and S4, each consisting of 15 Gaussian clusters in $\mathbb{R}^2$. Visualizations of S-sets are provided in Appendix C.

We assess recovered centroids by calculating the ℓ_2-distance to ground truth centers, with mean results and standard deviation from 10 runs reported in Table 1. Additionally, ~~standard deviations are detailed in ,~~

~~while~~ the Purity and NMI of clustering assignment quality are presented in subsection C.1. We focus on three data split conditions in the federated setting: IID, Dirichlet(0.3), and Dirichlet(0.1). And we select $k' = 5$ for k-FED after careful tuning (detailed in subsection C.5).

Results in Table 1 indicate that our algorithm FeCA consistently outperforms all baselines in recovering the global solution across all experimental settings. Figure 4 provides a visualization of these results, demonstrating that even under the challenging non-IID condition – Dirichlet(0.3), FeCA's recovered centroids closely approximate the true centers.

Table 1: **ℓ_2-distance (scaled by 10^4) between recovered centroids and true centers on S-sets under three data split conditions.** Dirichlet(0.3) and Dirichlet(0.1) are denoted as (0.3) and (0.1), respectively. *Rd* indicates rounds for FFCM. We report mean±std from 10 random runs.

ℓ_2-distance $\times 10^4$	S-sets (S1)			S-sets (S2)		
Method	IID	(0.3)	(0.1)	IID	(0.3)	(0.1)
M-Avg	7.2±4.3	45.8±5.0	63.0±2.8	14.7±7.1	51.4±8.9	64.0±11.1
FFCMv1(Rd=1)	12.2±15.8	80.7±13.3	81.1±15.7	16.7±20.4	70.9±13.3	89.7±16.0
FFCMv1(Rd=10)	3.3±1.4	50.3±8.8	66.1±12.4	9.6±19.1	56.9±12.3	60.3±18.2
FFCMv2(Rd=1)	23.1±19.4	75.7±16.8	77.0±14.4	16.1±16.9	71.9±13.5	79.9±12.6
FFCMv2(Rd=10)	2.6±0.4	42.9±14.8	54.2±14.6	32.9±0.5	58.1±13.5	59.4±25.8
k-FED(k'=5)	84.6±15.8	59.4±12.3	59.8±16.9	75.9±17.7	64.1±13.1	63.9±11.6
FeCA	**1.0**±0.1	**6.8**±3.7	**22.3**±15.6	**1.9**±0.1	**13.6**±16.1	**38.8**±3.4
Centralized		14.3±18.7			8.4±14.7	

ℓ_2-distance $\times 10^4$	S-sets (S3)			S-sets (S4)		
Method	IID	(0.3)	(0.1)	IID	(0.3)	(0.1)
M-Avg	16.4±6.8	35.5±5.7	46.7±5.3	14.2±3.7	28.7±3.3	40.1±6.4
FFCMv1(Rd=1)	16.6±15.2	58.1±11.9	77.4±8.9	11.4±9.5	45.0±8.9	63.1±10.8
FFCMv1(Rd=10)	11.4±15.5	45.9±8.8	66.6±12.9	4.8±1.3	45.0±12.3	52.0±11.9
FFCMv2(Rd=1)	18.2±12.6	62.7±12.6	79.1±10.2	13.0±11.4	48.9±9.7	60.4±9.6
FFCMv2(Rd=10)	4.5±0.7	49.4±19.3	56.7±16.7	4.9±0.6	44.6±9.1	49.9±7.3
k-FED(k'=5)	73.1±14.3	65.6±15.2	68.8±12.8	52.7±10.8	43.4±6.3	47.5±8.6
FeCA	**3.6**±0.7	**23.6**±8.8	**33.2**±6.7	**4.7**±0.7	**24.5**±7.2	**31.5**±5.8
Centralized		25.4±19.1			20.1±10.0	

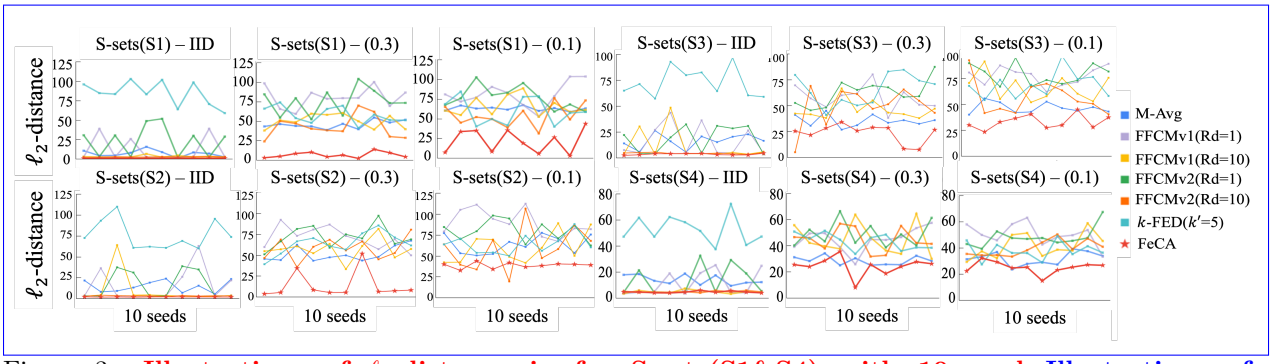

Figure 3: ~~**Illustrations of ℓ_2-distance in for S-sets(S1&S4) with 10 seeds.**~~**Illustrations of ℓ_2-distance in Table 1 for S-sets using 10 random seeds.**

Gain by playing the Jigsaw game. Table 1 reveals an interesting finding: FeCA (and some other federated clustering methods) can even outperform the centralized k-means. From the perspective of federated

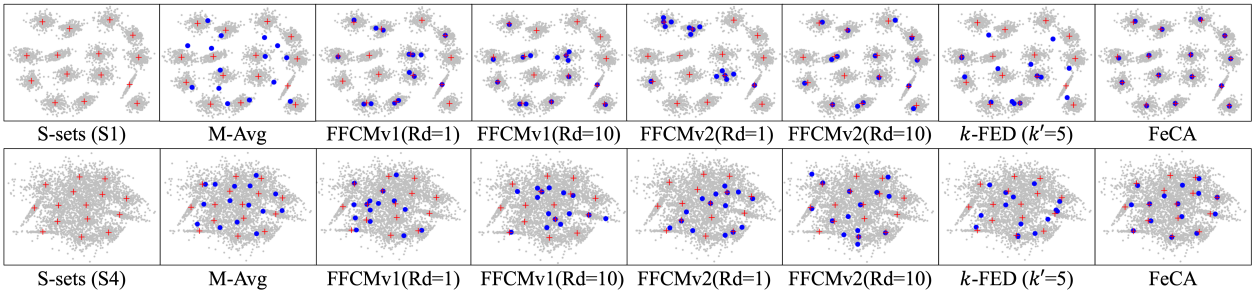

Figure 4: **Visualizations of S-sets (S1&S4) and recovered centroids by different methods.** Results are showcased under the Dirichlet(0.3) data split condition. Blue dots represent recovered centroids, and red crosses indicate the ground truth centers.

learning, this may look odd. But it makes perfect sense from the local solution point of view of k-means. Solving centralized k-means likely leads to a local solution with suboptimal performance. However, with multiple clients independently solving k-means, their solutions together have a higher chance to jointly reveal the global solution. To explore this gain by playing the jigsaw game on clients' solutions, we conduct experiments on the impact of varying numbers of clients on the synthetic dataset, as detailed in Appendix D.

On frozen features. We evaluate FeCA on features extracted from pre-trained neural networks using real datasets – CIFAR10/100 Krizhevsky et al. (2009). And the frozen features are generated from the ImageNet pre-trained ResNet-50 He et al. (2016) model. For k-FED algorithm, we select $k' = 3$ for CIFAR10 and $k' = 10$ for CIFAR100, following the suggestion $k' \leq \sqrt{k^*}$ from their paper. In Table 2, we present the average Purity and NMI calculated from three random runs. Our algorithm FeCA demonstrates robust performance across different data split conditions. And it outperforms all baseline models in most cases.

Under the extreme non-IID condition – Dirichlet(0.1), the k-FED algorithm tends to outperform others. This is because k-FED is designed for high heterogeneity, assuming each client possesses data from $k' \leq \sqrt{k^*}$ true clusters. Without considering local solution structures in k-means, k-FED relies on an accurate selection of k' to reduce the chance of occurrence of spurious centroids in scenarios of high heterogeneity, as illustrated in Figure 1(right). This strategy makes its performance highly sensitive to the choice of k', and it tends to decrease rapidly under less heterogeneous conditions. This situation highlights the importance of addressing local solutions in federated clustering.

Table 2: **Purity and NMI on CIFAR-10/100.** We present mean results from three random runs under four data split conditions. For k-FED method, we select k'=3 on CIFAR-10 and k'=10 on CIFAR-100.

	CIFAR-10								CIFAR-100							
	Purity				NMI				Purity				NMI			
Method	IID	(1.0)	(0.3)	(0.1)	IID	(1.0)	(0.3)	(0.1)	IID	(1.0)	(0.3)	(0.1)	IID	(1.0)	(0.3)	(0.1)
M-Avg	0.48	0.45	0.41	0.39	0.43	0.41	0.35	0.34	0.20	0.19	0.19	0.18	0.37	0.37	0.36	0.36
FFCMv1(Rd=1)	0.24	0.32	0.37	0.36	0.33	0.37	0.38	0.36	0.06	0.07	0.07	0.07	0.24	0.25	0.24	0.25
FFCMv1(Rd=10)	0.20	0.20	0.23	0.24	0.31	0.31	0.32	0.31	0.03	0.03	0.04	0.03	0.13	0.13	0.15	0.14
FFCMv2(Rd=1)	0.32	0.44	0.53	0.56	0.27	0.43	0.48	0.50	0.10	0.11	0.11	0.12	0.27	0.30	0.30	0.32
FFCMv2(Rd=10)	0.32	0.43	0.53	0.56	0.27	0.43	0.48	0.50	0.10	0.10	0.10	0.12	0.26	0.28	0.29	0.31
k-FED	0.28	0.41	0.47	0.51	0.30	0.39	0.47	**0.52**	0.10	0.22	0.34	**0.48**	0.27	0.37	0.49	**0.62**
FeCA	**0.61**	**0.60**	**0.58**	**0.57**	**0.53**	**0.51**	**0.49**	0.50	**0.37**	**0.37**	**0.37**	0.34	**0.49**	**0.49**	**0.49**	0.47
Centralized	0.64				0.53				0.39				0.50			

Table 3: **Top-1 test accuracy (%) with linear evaluation.** We present mean results from 3 runs on three datasets.

Accuracy (%)	CIFAR-10			CIFAR-100			Tiny-ImageNet		
Method	IID	(0.3)	(0.1)	IID	(0.3)	(0.1)	IID	(0.3)	(0.1)
M-Avg	53.6	48.2	45.1	25.2	24.8	23.6	16.4	15.1	13.5
FFCMv1(Rd=1)	44.6	48.5	45.5	22.5	25.0	25.9	12.1	16.9	12.5
FFCMv2(Rd=1)	47.7	50.1	49.1	21.9	22.9	22.9	14.9	14.1	14.0
k-FED(k'=20)	46.8	50.0	47.1	27.5	28.9	29.7	15.3	18.9	23.4
DeepFeCA	**55.3**	**63.7**	**59.9**	**35.3**	**34.9**	**35.2**	**26.7**	**26.4**	**26.1**
Centralized	80.9			50.1			36.6		

6.2 DeepFeCA Evaluation

We validate DeepFeCA on the CIFAR10/100 and the Tiny-ImageNet dataset with 64×64 resolution. We randomly initialize a ResNet-18 model and train it for 150 rounds, with all 10 clients fully participating in the process. Each round we train 5 local epochs for clients' models with batch size 128. We modified the official implementation of DeepCluster-v2 Caron et al. (2020) and followed their training details.

The test accuracy is reported using linear evaluation, with the mean results of three runs presented in Table 3. Since FFCM requires one communication between the server and clients for each round, we only perform FFCM(Rd=1) given the computation resource constraint. And we set $k' = 20$ for k-FED on Tiny-ImageNet. We first confirm that the centralized training of DeepCluster-v2 reaches reasonable accuracy on three datasets. Also, we see that the performance in federated framework drops sharply compared to centralized learning, showing the challenges of learning deep representation on decentralized data. One possible reason could be the limited performance of k-means clustering results on noisy features, especially in the early rounds, leading to unreliable pseudo labels in the following supervised training step.

However, our method shows encouraging improvements. The DeepFeCA outperforms the baselines significantly and consistently across all settings on three datasets. From experiments, we demonstrate: (1) it is challenging for DeepFeCA-v2 in federated settings to match its centralized performance; (2) it is possible for the current baseline to learn meaningful features in federated settings; (3) the proposed DeepFeCA serves as a strong baseline, which outperforms current algorithms by a notable gain.

7 Conclusions

We investigate federated clustering, an important yet underexplored area in federated unsupervised learning, and propose a novel one-shot algorithm, FeCA, which adopts an innovative approach by utilizing structures of local solutions in k-means. We also adapt FeCA for representation learning and propose DeepFeCA. Through comprehensive experiments on benchmark datasets, both FeCA and DeepFeCA demonstrate superior performance and robustness, outperforming established baselines across various settings.

References

Yuki Markus Asano, Christian Rupprecht, and Andrea Vedaldi. Self-labelling via simultaneous clustering and representation learning. In *ICLR*, 2020.

Olivier Bachem, Mario Lucic, and Andreas Krause. Scalable k-means clustering via lightweight coresets. In *Proceedings of the 24th ACM SIGKDD International Conference on Knowledge Discovery & Data Mining*, pp. 1119–1127, 2018.

Maria-Florina F Balcan, Steven Ehrlich, and Yingyu Liang. Distributed k-means and k-median clustering on general topologies. In C. J. C. Burges, L. Bottou, M. Welling, Z. Ghahramani, and K. Q. Weinberger (eds.), *Advances in Neural Information Processing Systems*. Curran Associates, Inc., 2013.

Mathilde Caron, Piotr Bojanowski, Armand Joulin, and Matthijs Douze. Deep clustering for unsupervised learning of visual features. In *Proceedings of the European Conference on Computer Vision (ECCV)*, pp. 132–149, 2018.

Mathilde Caron, Ishan Misra, Julien Mairal, Priya Goyal, Piotr Bojanowski, and Armand Joulin. Unsupervised learning of visual features by contrasting cluster assignments. *arXiv preprint arXiv:2006.09882*, 2020.

Hong-You Chen and Wei-Lun Chao. Fedbe: Making bayesian model ensemble applicable to federated learning. In *ICLR*, 2021.

Yudong Chen and Xumei Xi. Likelihood landscape and local minima structures of Gaussian mixture models. *arXiv preprint arxiv:2009.13040*, 2020.

Liam Collins, Hamed Hassani, Aryan Mokhtari, and Sanjay Shakkottai. Exploiting shared representations for personalized federated learning. 2021.

Don Kurian Dennis, Tian Li, and Virginia Smith. Heterogeneity for the win: One-shot federated clustering. *arXiv preprint arXiv:2103.00697*, 2021.

Ahmed Elhussein and Gamze Gürsoy. Privacy-preserving patient clustering for personalized federated learnings. In *Machine Learning for Healthcare Conference*, pp. 150–166. PMLR, 2023.

Linus Ericsson, Henry Gouk, and Timothy M Hospedales. How well do self-supervised models transfer? In *CVPR*, pp. 5414–5423, 2021.

Pasi Fränti and Sami Sieranoja. K-means properties on six clustering benchmark datasets, 2018. URL `http://cs.uef.fi/sipu/datasets/`.

Avishek Ghosh, Jichan Chung, Dong Yin, and Kannan Ramchandran. An efficient framework for clustered federated learning. *Advances in Neural Information Processing Systems*, 33:19586–19597, 2020.

Andrey Goder and Vladimir Filkov. Consensus clustering algorithms: Comparison and refinement. In *2008 Proceedings of the Tenth Workshop on Algorithm Engineering and Experiments (ALENEX)*, pp. 109–117. SIAM, 2008.

Farzin Haddadpour and Mehrdad Mahdavi. On the convergence of local descent methods in federated learning. *arXiv preprint arXiv:1910.14425*, 2019.

Chaoyang He, Murali Annavaram, and Salman Avestimehr. Group knowledge transfer: Federated learning of large cnns at the edge. In *NeurIPS*, 2020.

Kaiming He, Xiangyu Zhang, Shaoqing Ren, and Jian Sun. Deep residual learning for image recognition. In *CVPR*, 2016.

Tom Hess, Ron Visbord, and Sivan Sabato. Fast distributed k-means with a small number of rounds. *arXiv preprint arXiv:2201.13217*, 2022.

Jiazhen Hong, Wei Qian, Yudong Chen, and Yuqian Zhang. A geometric approach to k-means. *arXiv preprint arXiv:2201.04822*, 2022.

Tzu-Ming Harry Hsu, Hang Qi, and Matthew Brown. Measuring the effects of non-identical data distribution for federated visual classification. *arXiv preprint arXiv:1909.06335*, 2019.

Eshref Januzaj, Hans-Peter Kriegel, and Martin Pfeifle. Dbdc: Density based distributed clustering. In *International Conference on Extending Database Technology*, pp. 88–105. Springer, 2004.

Wonyong Jeong, Jaehong Yoon, Eunho Yang, and Sung Ju Hwang. Federated semi-supervised learning with inter-client consistency & disjoint learning. 2020.

Amelia Jiménez-Sánchez, Mickael Tardy, Miguel A González Ballester, Diana Mateus, and Gemma Piella. Memory-aware curriculum federated learning for breast cancer classification. *Computer Methods and Programs in Biomedicine*, 229:107318, 2023.

Hillol Kargupta, Weiyun Huang, Krishnamoorthy Sivakumar, and Erik Johnson. Distributed clustering using collective principal component analysis. *Knowledge and Information Systems*, 3(4):422–448, 2001.

A Khaled, K Mishchenko, and P Richtárik. Tighter theory for local sgd on identical and heterogeneous data. In *AISTATS*, 2020.

Alex Krizhevsky, Geoffrey Hinton, et al. Learning multiple layers of features from tiny images. 2009.

Ya Le and Xuan Yang. Tiny imagenet visual recognition challenge. *CS 231N*, 2015.

Guangrui Li, Guoliang Kang, Yi Zhu, Yunchao Wei, and Yi Yang. Domain consensus clustering for universal domain adaptation. In *Proceedings of the IEEE/CVF conference on computer vision and pattern recognition*, pp. 9757–9766, 2021.

Songze Li, Sizai Hou, Baturalp Buyukates, and Salman Avestimehr. Secure federated clustering. *arXiv preprint arXiv:2205.15564*, 2022.

Yiwei Li, Shuai Wang, Chong-Yung Chi, and Tony QS Quek. Differentially private federated clustering over non-iid data. *arXiv preprint arXiv:2301.00955*, 2023.

Tao Lin, Lingjing Kong, Sebastian U Stich, and Martin Jaggi. Ensemble distillation for robust model fusion in federated learning. In *NeurIPS*, 2020.

Xiao Liu, Fanjin Zhang, Zhenyu Hou, Li Mian, Zhaoyu Wang, Jing Zhang, and Jie Tang. Self-supervised learning: Generative or contrastive. *IEEE Transactions on Knowledge and Data Engineering*, 2021.

Stuart Lloyd. Least squares quantization in pcm. *IEEE transactions on information theory*, 28(2):129–137, 1982.

Guodong Long, Ming Xie, Tao Shen, Tianyi Zhou, Xianzhi Wang, and Jing Jiang. Multi-center federated learning: clients clustering for better personalization. *World Wide Web*, 26(1):481–500, 2023.

Lin Lu, Yao Lin, Yuan Wen, Jinxiong Zhu, and Shengwu Xiong. Federated clustering for recognizing driving styles from private trajectories. *Engineering Applications of Artificial Intelligence*, 118:105714, 2023.

Ekdeep Singh Lubana, Chi Ian Tang, Fahim Kawsar, Robert P Dick, and Akhil Mathur. Orchestra: Unsupervised federated learning via globally consistent clustering. *arXiv preprint arXiv:2205.11506*, 2022.

Brendan McMahan, Eider Moore, Daniel Ramage, Seth Hampson, and Blaise Aguera y Arcas. Communication-efficient learning of deep networks from decentralized data. In *Artificial intelligence and statistics*, pp. 1273–1282. PMLR, 2017.

Stefano Monti, Pablo Tamayo, Jill Mesirov, and Todd Golub. Consensus clustering: a resampling-based method for class discovery and visualization of gene expression microarray data. *Machine learning*, 52(1): 91–118, 2003.

Jaehoon Oh, Sangmook Kim, and Se-Young Yun. Fedbabu: Towards enhanced representation for federated image classification. *arXiv preprint arXiv:2106.06042*, 2021.

Wei Qian, Yuqian Zhang, and Yudong Chen. Structures of spurious local minima in k-means. *IEEE Transactions on Information Theory*, 68(1):395–422, 2021.

Cheng Qiao, Kenneth N Brown, Fan Zhang, and Zhihong Tian. Federated adaptive asynchronous clustering algorithm for wireless mesh networks. *IEEE Transactions on Knowledge and Data Engineering*, 2021.

Morris Stallmann and Anna Wilbik. Towards federated clustering: A federated fuzzy c-means algorithm (ffcm). *arXiv preprint arXiv:2201.07316*, 2022.

Yue Tan, Yixin Liu, Guodong Long, Jing Jiang, Qinghua Lu, and Chengqi Zhang. Federated learning on non-iid graphs via structural knowledge sharing. In *Proceedings of the AAAI conference on artificial intelligence*, volume 37, pp. 9953–9961, 2023.

Hongyi Wang, Mikhail Yurochkin, Yuekai Sun, Dimitris Papailiopoulos, and Yasaman Khazaeni. Federated learning with matched averaging. In *ICLR*, 2020.

Chang Xia, Jingyu Hua, Wei Tong, and Sheng Zhong. Distributed k-means clustering guaranteeing local differential privacy. *Computers & Security*, 90:101699, 2020.

Mikhail Yurochkin, Mayank Agarwal, Soumya Ghosh, Kristjan Greenewald, Trong Nghia Hoang, and Yasaman Khazaeni. Bayesian nonparametric federated learning of neural networks. In *ICML*, 2019.

Dun Zeng, Siqi Liang, Xiangjing Hu, Hui Wang, and Zenglin Xu. Fedlab: A flexible federated learning framework. *Journal of Machine Learning Research*, 24(100):1–7, 2023.

Fengda Zhang, Kun Kuang, Long Chen, Zhaoyang You, Tao Shen, Jun Xiao, Yin Zhang, Chao Wu, Fei Wu, Yueting Zhuang, et al. Federated unsupervised representation learning. *Frontiers of Information Technology & Electronic Engineering*, 24(8):1181–1193, 2023a.

Jianqing Zhang, Yang Hua, Hao Wang, Tao Song, Zhengui Xue, Ruhui Ma, and Haibing Guan. Fedala: Adaptive local aggregation for personalized federated learning. In *Proceedings of the AAAI Conference on Artificial Intelligence*, volume 37, pp. 11237–11244, 2023b.

Zhengming Zhang, Yaoqing Yang, Zhewei Yao, Yujun Yan, Joseph E Gonzalez, and Michael W Mahoney. Improving semi-supervised federated learning by reducing the gradient diversity of models. *arXiv preprint arXiv:2008.11364*, 2020.

Yanlin Zhou, George Pu, Xiyao Ma, Xiaolin Li, and Dapeng Wu. Distilled one-shot federated learning. *arXiv preprint arXiv:2009.07999*, 2020.

Weiming Zhuang, Xin Gan, Yonggang Wen, Shuai Zhang, and Shuai Yi. Collaborative unsupervised visual representation learning from decentralized data. In *Proceedings of the IEEE/CVF International Conference on Computer Vision*, pp. 4912–4921, 2021.

A Proof of Theorem 4.1

In this section, we prove Theorem 4.1, which states that under the Stochastic Ball Model and high Signal-to-Noise Ratios (SNR) condition, all the clients returned one/many-fit-one centroids corresponding to the same ground truth center are bounded within a ball of some radius (determined by Algorithm 3). Furthermore, for the final output centroids $\mathcal{C}^* = \{c_1^*, \ldots, c_k^*\}$ from our main Algorithm 1, we demonstrate that the distance between each centroid $c_s^* \in \mathcal{C}^*, s \in [k]$ and its corresponding true center θ_s^* is upper bounded. Specifically, the proof can be composed of the following three steps:

- **Step 1 (Proof of the effectiveness of removing one-fit-many in Algorithm 2)**: On the client end, we prove the effectiveness of removing all one-fit-many centroids by Algorithm 2;
- **Step 2 (Proof of the effectiveness of assigning radius in Algorithm 3)**: On the server end, we prove that the radius assigned by Algorithm 3 effectively encloses all the centroids (returned from the clients) associated to the same true center;
- **Step 3 (Proof of Theorem 4.1)**: On the server end, under the assumption that there does not exist any one-fit-many centroid (proved in Step 1), we first prove Algorithm 5 correctly classifies all the returned centroids $\mathcal{C} = \{\mathcal{C}^{(1)}, \ldots, \mathcal{C}^{(M)}\}$ from M clients using radii assigned by Algorithm 3, and then derive the error bound between recovered centroids and ground truth centers.

We first introduce some notations used in the following proof and a formal description of the Stochastic Ball Model below.

Stochastic Ball Model and Notations. Let $\theta_1^*, \ldots, \theta_k^* \in \mathbb{R}^d$ represent k distinct true cluster centers, and f_s be the density of a distribution with mean θ_s^* for each $s \in [k]$. We assume each data point $x^{(m)} \in \mathbb{R}^d$ of client $m \in [M]$ is sampled independently and uniformly from a mixture f of distributions $\{f_s\}_{s\in[k]}$, with the density

$$f(x) = \frac{1}{k}\sum_{s=1}^{k} f_s(x). \tag{7}$$

The Stochastic Ball Model is the mixture f where each ball component has density

$$f_s(x) = \frac{1}{\mathrm{Vol}(\mathbb{B}_s)}\mathbb{1}_{\mathbb{B}_s}(x), \quad s \in [k], \tag{8}$$

where $\mathbb{B}_s$ denotes a ball component centered at θ_s^* with radius r. In the context of the k-means problem, to identify a set of k centroids $\mathcal{C}^{(m)} = \{c_1^{(m)}, \ldots, c_k^{(m)}\}$ on client m, we consider the goal as minimizing the following objective:

$$G(\mathcal{C}^{(m)}) = \int \min_{i\in[k]} \|x^{(m)} - c_i^{(m)}\|_2^2 f(x^{(m)})dx^{(m)} = \frac{1}{k}\sum_{s=1}^{k}\int \min_{i\in[k]} \|x^{(m)} - c_i^{(m)}\|_2^2 f_s(x^{(m)})dx^{(m)}. \tag{9}$$

The above objective function represents the infinite-sample ($n \to \infty$) limit of the empirical objective function in Equation 1. We note that this objective is still non-convex. The associated clusters of centroids $\mathcal{C}^{(m)}$ are denoted as $\mathcal{D}^{(m)} = \{\mathcal{D}_1^{(m)}, \ldots, \mathcal{D}_k^{(m)}\}$. In addition, we define the maximum and minimum pairwise separations between true centers $\{\theta_s^*\}_{s\in[k]}$ as

$$\Delta_{max} := \max_{s\neq s'} \|\theta_s^* - \theta_{s'}^*\|_2 \qquad \text{and} \qquad \Delta_{min} := \min_{s\neq s'} \|\theta_s^* - \theta_{s'}^*\|_2. \tag{10}$$

A.1 Step 1 (Proof of the effectiveness of removing one-fit-many in Algorithm 2)

In this section, we prove the effectiveness of Algorithm 2 in eliminating all one-fit-many centroids under the Stochastic Ball Model. Specifically, on each client $m \in [M]$, Lloyd's algorithm is deployed on clients' data $x_1^{(m)}, \ldots, x_n^{(m)} \in \mathbb{R}^d$ to obtain k clusters $\mathcal{D}^{(m)} = \{\mathcal{D}_1^{(m)}, \ldots, \mathcal{D}_k^{(m)}\}$ and corresponding k centroids $\mathcal{C}^{(m)} = \{c_1^{(m)}, \ldots, c_k^{(m)}\}$. If $\mathcal{C}^{(m)}$ is a non-degenerate local minimum that is not the global optimum, then it must contain both one-fit-many and many-fit-one centroids, as discussed in subsection 3.1.

Next, the algorithm identifies a candidate one-fit-many centroid $c_i^{(m)} \in \mathcal{C}^{(m)}$ whose corresponding cluster $\mathcal{D}_i^{(m)}$ has the largest standard deviation, and then computes the objective value $G_i^{(m)}$ for this cluster $\mathcal{D}_i^{(m)}$ as detailed in Equation 3. In this proof, we focus on the infinite-sample case ($n \to \infty$) and derive $G_i^{(m)}$ as

$$G_i^{(m)} = \int_{\mathcal{D}_i^{(m)}} \|x - c_i^{(m)}\|_2^2 f(x)dx. \tag{11}$$

In addition, the algorithm pinpoints two candidate many-fit-one centroids $c_p^{(m)}$ and $c_q^{(m)}$ from $\mathcal{C}^{(m)}$, characterized by the minimal pairwise distance. Then we tentatively merge the respective clusters $\mathcal{D}_p^{(m)}$ and $\mathcal{D}_q^{(m)}$ of $c_p^{(m)}$ and $c_q^{(m)}$ to form a new cluster $\mathcal{D}_j^{(m)}$ and then obtain a new centroid $c_j^{(m)}$. Subsequently, the objective value $G_j^{(m)}$ for cluster $\mathcal{D}_j^{(m)}$ as $n \to \infty$ is calculated as

$$G_j^{(m)} = \int_{\mathcal{D}_j^{(m)}} \|x - c_j^{(m)}\|_2^2 f(x)dx, \quad \text{where} \quad \mathcal{D}_j^{(m)} = \mathcal{D}_p^{(m)} \cup \mathcal{D}_q^{(m)}. \tag{12}$$

To test if these candidate centroids $c_i^{(m)}$ and $\{c_p^{(m)}, c_q^{(m)}\}$ are one-fit-many and many-fit-one centroids, Algorithm 2 compares $G_i^{(m)}$ and $G_j^{(m)}$. If $G_i^{(m)} \geq G_j^{(m)}$, then $c_i^{(m)}$ is a one-fit-many centroid to be removed and $\{c_p^{(m)}, c_q^{(m)}\}$ are many-fit-one centroids to be kept. This is proved in Lemma A.1.

Lemma A.1. *Under the Stochastic Ball Model, for some constants $\lambda \geq 3$ and $\eta \geq 5$, if*

$$\Delta_{max} \geq 4\lambda^2 k^4 r \qquad \text{and} \qquad \Delta_{min} \geq 10\eta\lambda k^2 \sqrt{r\Delta_{max}}, \tag{13}$$

then Algorithm 2 eliminates all existing one-fit-many centroids from the local minimizer $\mathcal{C}^{(m)}$ on client m.

Proof. If $\mathcal{C}^{(m)}$ is a non-degenerate local minimum that is not globally optimal on client m, then it must contain both one-fit-many and many-fit-one centroids. Without loss of generality, assume that $c_i^{(m)} \in \mathcal{C}^{(m)}$ is associated with multiple true centers $\theta_1^*, \ldots, \theta_t^*$, where $t \geq 2$. Additionally, let $\{c_p^{(m)}, c_q^{(m)}\} \in \mathcal{C}^{(m)}$ (potentially along with other centroids) are associated with the same true center θ_{t+1}^*. Then the objective $G^{(m)}$ of $\mathcal{C}^{(m)}$ is

$$G^{(m)} = G_i^{(m)} + T_1 + B, \quad \text{where} \quad T_1 = \int_{\mathcal{D}_p^{(m)} \cup \mathcal{D}_q^{(m)}} \min\{\|x - c_p^{(m)}\|_2^2, \|x - c_q^{(m)}\|_2^2\} f(x)dx, \tag{14}$$

and $G_i^{(m)}$ is the objective of $\mathcal{D}_i^{(m)}$ as defined in (11). B denotes the objective value contributed from data points from clusters other than $\{\mathcal{D}_i^{(m)}, \mathcal{D}_p^{(m)}, \mathcal{D}_q^{(m)}\}$.

We construct a hypothetical solution $\mathcal{C}_h^{(m)}$ by: (1) merging clusters $\mathcal{D}_p^{(m)}$ and $\mathcal{D}_q^{(m)}$ into a single cluster $\mathcal{D}_j^{(m)}$ with a new centroid $c_j^{(m)}$; (2) dividing the cluster $\mathcal{D}_i^{(m)}$ into two clusters $\mathcal{D}_{i_1}^{(m)}$ and $\mathcal{D}_{i_2}^{(m)}$, with centroids $c_{i_1}^{(m)}$ and $c_{i_2}^{(m)}$ respectively; (3) keeping the remaining centroids in $\mathcal{C}^{(m)}$. Thus, we have

$$\mathcal{C}_h^{(m)} = \mathcal{C}^{(m)} \setminus \{c_i^{(m)}, c_p^{(m)}, c_q^{(m)}\} \cup \{c_{i_1}^{(m)}, c_{i_2}^{(m)}, c_j^{(m)}\}. \tag{15}$$

The objective $G_h^{(m)}$ for this hypothetical solution $\mathcal{C}_h^{(m)}$ is

$$G_h^{(m)} = G_j^{(m)} + T_2 + B, \quad \text{where} \quad T_2 = \int_{\mathcal{D}_i^{(m)}} \min\{\|x - c_{i_1}^{(m)}\|_2^2, \|x - c_{i_2}^{(m)}\|_2^2\} f(x)dx, \tag{16}$$

and $G_j^{(m)}$ is the objective value for the merged cluster $\mathcal{D}_j^{(m)}$ as defined in (12). By selecting centroids $c_{i_1}^{(m)} = c_i^{(m)}$ and $c_{i_2}^{(m)} = \arg\max_{x \in \mathcal{D}_i^{(m)}} \|x - c_i^{(m)}\|$ and Lemma A.2, we have

$$G^{(m)} - G_h^{(m)} \geq \frac{\Delta_{min}^2}{36k}. \tag{17}$$

This inequality implies that $\mathcal{C}^{(m)}$ is a local solution with a suboptimal objective value $G^{(m)}$. In Algorithm 2, instead of comparing $G^{(m)}$ and $G_h^{(m)}$, we evaluate $G_i^{(m)}$ and $G_j^{(m)}$ to determine whether $\mathcal{C}^{(m)}$ is a local solution. The difference between objective values $G^{(m)}$ and $G_h^{(m)}$ is

$$G^{(m)} - G_h^{(m)} = G_i^{(m)} - G_j^{(m)} - (T_2 - T_1). \tag{18}$$

Note that the term T_2 is the objective value of two splitted clusters $\mathcal{D}_{i_1}^{(m)}$ and $\mathcal{D}_{i_2}^{(m)}$. Following the selection of centroids $c_{i_1}^{(m)}$ and $c_{i_2}^{(m)}$ as above, we have the proved claim that $\|c_{i_1}^{(m)} - c_{i_2}^{(m)}\| \geq \frac{\Delta_{min}}{2} - r$ from the proof

of Lemma A.2 in Hong et al. (2022). It follows that

$$T_2 = \int_{\mathcal{D}_{i_1}^{(m)}} \|x - c_{i_1}^{(m)}\|_2^2 f(x)dx + \int_{\mathcal{D}_{i_2}^{(m)}} \|x - c_{i_2}^{(m)}\|_2^2 f(x)dx \tag{19}$$

$$\geq \int_{\mathcal{D}_{i_2}^{(m)}} \left(\|c_{i_1}^{(m)} - c_{i_2}^{(m)}\|_2 - \|x - c_{i_1}^{(m)}\|_2\right)^2 f(x)dx \tag{20}$$

$$\geq \int_{\mathcal{D}_{i_2}^{(m)}} \left(\frac{\Delta_{min}}{2} - r - 2r\right)^2 f(x)dx \tag{21}$$

$$\geq \frac{1}{k}\left(\frac{\Delta_{min}}{2} - 3r\right)^2 \tag{22}$$

$$\geq \frac{1}{k}\left(\frac{2\Delta_{min}}{5}\right)^2 \tag{23}$$

Equation (19) follows from $\mathcal{D}_i^{(m)} = \mathcal{D}_{i_1}^{(m)} \cup \mathcal{D}_{i_2}^{(m)}$. Inequality (20) uses the triangle inequality, and (21) follows from the choice of $c_{i_1}^{(m)}$ and $c_{i_2}^{(m)}$. Inequality (22) stems from the ball component's volume being $\frac{1}{k}$. Inequality (23) follows the claim that $r \leq \frac{\Delta_{min}}{20\eta\lambda^2k^4} \leq \frac{\Delta_{min}}{30}$, which is derived from the separation assumption in (13).

For the term T_1, we have

$$T_1 = \int_{\mathcal{D}_p^{(m)}} \|x - c_p^{(m)}\|_2^2 f(x)dx + \int_{\mathcal{D}_q^{(m)}} \|x - c_q^{(m)}\|_2^2 f(x)dx \tag{24}$$

$$\leq \int_{\mathcal{D}_p^{(m)}} \left(\|x - \theta_{t+1}^*\|_2 + \|\theta_{t+1}^* - c_p^{(m)}\|_2\right)^2 f(x)dx + \int_{\mathcal{D}_q^{(m)}} \left(\|x - \theta_{t+1}^*\|_2 + \|\theta_{t+1}^* - c_q^{(m)}\|_2\right)^2 f(x)dx \tag{25}$$

$$\leq \int_{\mathcal{D}_p^{(m)}} \left(r + 8\lambda k^2\sqrt{r\Delta_{max}}\right)^2 f(x)dx + \int_{\mathcal{D}_q^{(m)}} \left(r + 8\lambda k^2\sqrt{r\Delta_{max}}\right)^2 f(x)dx \tag{26}$$

$$= \int_{\mathcal{D}_j^{(m)}} \left(r + 8\lambda k^2\sqrt{r\Delta_{max}}\right)^2 f(x)dx \leq \frac{1}{k}\left(r + \frac{4\Delta_{min}}{5\eta}\right)^2 \leq \frac{1}{k}\left(\frac{\Delta_{min}}{3}\right)^2 \tag{27}$$

Equation (24) follows from the definition of the term T_1. Inequality (25) follows from the triangle inequality. Inequality (26) utilizes the error bound from Theorem 1 (many/one-fit-one association) in Qian et al. (2021), considering each ball component's radius as r. Inequality (27) is based on the volume of each ball component being $\frac{1}{k}$, the proved claim $r \leq \frac{\Delta_{min}}{30}$, and the assumption that $\eta \geq 5$.

Combining the above inequalities, we have $T_2 - T_1 \geq 0$. Thus, the equation (18) can be derived as

$$G_i^{(m)} - G_j^{(m)} = G^{(m)} - G_h^{(m)} + (T_2 - T_1) \geq G^{(m)} - G_h^{(m)} \geq \frac{\Delta_{min}^2}{36k} \geq 0. \tag{28}$$

Therefore, if $G_i^{(m)} \geq G_j^{(m)}$, it implies that $\mathcal{C}^{(m)}$ is a local solution with a suboptimal objective value $G^{(m)}$. Subsequently, by comparing $G_i^{(m)}$ and $G_j^{(m)}$ for each candidate centroid $c_i^{(m)}$, Algorithm 2 can effectively eliminates all one-fit-many centroids from $\mathcal{C}^{(m)}$. □

Lemma A.2. *Under the Stochastic Ball Model, for some constants $\lambda \geq 3$ and $\eta \geq 5$, if*

$$\Delta_{max} \geq 4\lambda^2k^4r \qquad \textit{and} \qquad \Delta_{min} \geq 10\eta\lambda k^2\sqrt{r\Delta_{max}}, \tag{29}$$

then when $c_{i_1}^{(m)} = c_i^{(m)}$ and $c_{i_2}^{(m)} = \arg\max_{x \in \mathcal{D}_i^{(m)}} \|x - c_i^{(m)}\|$, the following holds:

$$G^{(m)} - G_h^{(m)} \geq \frac{\Delta_{min}^2}{36k}. \tag{30}$$

Proof. The difference between objective values of the original solution $C^{(m)}$ and the hypothetical solution $C_h^{(m)}$ is

$$G^{(m)} - G_h^{(m)} = (G_i^{(m)} - T_2) - (G_j^{(m)} - T_1). \tag{31}$$

Lemma A.2 in Hong et al. (2022) establishes that by choosing centroids $c_{i_1}^{(m)} = c_i^{(m)}$ and $c_{i_2}^{(m)} = \arg\max_{x \in \mathcal{D}_i^{(m)}} \|x - c_i^{(m)}\|$, we have

$$G_i^{(m)} - T_2 \geq \frac{|D_{i_2}^{(m)}|}{n} \cdot \frac{1}{18}\Delta_{min}^2, \quad \text{and} \quad G_j^{(m)} - T_1 \leq \frac{|\mathcal{D}_j^{(m)}|}{n} \cdot (2r)^2, \tag{32}$$

where n is the total number of data points on client m and r is the radius of mixture ball components. This result is built on the objective in Equation 1 under the Stochastic Ball Model. Consider the objective function in (9) with the infinite-sample limit, we obtain

$$G_i^{(m)} - T_2 \geq \frac{\Delta_{min}^2}{18k}, \quad \text{and} \quad G_j^{(m)} - T_1 \leq \frac{4r^2}{k}. \tag{33}$$

It follows from as $n \to \infty$, $\frac{|\mathcal{D}_{i_2}^{(m)}|}{n}$ and $\frac{|\mathcal{D}_j^{(m)}|}{n}$ in (32) represent volumes of the ball components under the Stochastic Ball Model, each equating to $\frac{1}{k}$. Then, we derive

$$G^{(m)} - G_h^{(m)} \geq \frac{\Delta_{min}^2}{18k} - \frac{4r^2}{k} \geq \frac{\Delta_{min}^2}{36k}. \tag{34}$$

The second inequality in (34) follows the claim that $r \leq \frac{\Delta_{min}}{20\eta\lambda^2k^4} \leq \frac{\Delta_{min}}{30}$, which is derived from the separation assumption in (29).

□

A.2 Step 2 (Proof of the effectiveness of assigning radius in Algorithm 3)

In this section, we present a theoretical analysis demonstrating the effectiveness of the radius assignment in Algorithm 3, ensuring coverage of all centroids associated with one true center. On one hand, following the removal of all one-fit-many centroids by Algorithm 2 (proved in step 1), all returned centroids $\mathcal{C} = \{\mathcal{C}^{(1)}, \ldots, \mathcal{C}^{(M)}\}$ on the server end are concentrated around true centers $\{\theta_s^*\}_{s\in[k]}$. Thus, this is equivalently another clustering problem on centroids $\mathcal{C}$ with the high SNR separation condition. Let $\{\mathcal{S}_1^*, \ldots, \mathcal{S}_k^*\}$ be the ground truth clustering sets of all returned centroids $\mathcal{C}$, where for each $s \in [k]$, centroids within $\mathcal{S}_s^*$ are all associated with the one true center θ_s^*. Algorithm 5 classifies these returned centroids $\mathcal{C}$ into k sets $\{\mathcal{S}_1, \ldots, \mathcal{S}_k\}$, using the radius in $\mathcal{R} = \{\mathcal{R}^{(1)}, \ldots, \mathcal{R}^{(M)}\}$ determined by Algorithm 3.

On each client $m \in [M]$, Algorithm 3 first generates a new set of centroids $\tilde{\mathcal{C}}^{(m)}$ by discarding any potential many-fit-one centroid from $\mathcal{C}^{(m)}$. It then identifies the minimal pairwise distance $\tilde{\Delta}_{min}^{(m)}$ in $\tilde{\mathcal{C}}^{(m)}$ aiming to approximate Δ_{min}, formulated as:

$$\tilde{\Delta}_{min}^{(m)} = \min_{\tilde{c}_i, \tilde{c}_j \in \tilde{\mathcal{C}}^{(m)}, i \neq j} \|\tilde{c}_i - \tilde{c}_j\|_2. \tag{35}$$

Subsequently, Algorithm 3 calculates a uniform radius $r^{(m)} = \frac{1}{2}\tilde{\Delta}_{min}^{(m)}$, and assigns it to every centroid in $\mathcal{C}^{(m)}$. These centroid-radius pairs are then sent to the server.

Lemma A.3. *Under the Stochastic Ball Model, for some constant $\lambda \geq 3$ and $\eta \geq 5$, if*

$$\Delta_{max} \geq 4\lambda^2k^4r \qquad \text{and} \qquad \Delta_{min} \geq 10\eta\lambda k^2\sqrt{r\Delta_{max}}, \tag{36}$$

then for centroids in $\mathcal{S}_s^*$ which are associated with one true center $\theta_s^*, s \in [k]$, we have the following inequality holds on all clients $m \in [M]$:

$$\max_{c_i, c_j \in \mathcal{S}_s^*, i \neq j} \|c_j - c_i\|_2 \leq \frac{1}{2}\tilde{\Delta}_{min}^{(m)}, \quad \forall s \in [k]. \tag{37}$$

Proof. For centroids in $\mathcal{S}_s^*$ which are associated with one true center $\theta_s^*, s \in [k]$, we upper bound their maximum pairwise distance using the triangle inequality:

$$\begin{aligned}\max_{c_i,c_j\in\mathcal{S}_s^*,i\neq j}\|c_j-c_i\|_2 &\leq \max_{c_i,c_j\in\mathcal{S}_s^*,i\neq j}(\|c_j-\theta_s^*\|_2+\|\theta_s^*-c_i\|_2)\\ &\leq\ 2\max_{c_i\in\mathcal{S}_s^*}\|c_i-\theta_s^*\|_2. \end{aligned}\tag{38}$$

Under the Stochastic Ball Model with radius r, we apply the error bound from Theorem 1 (many/one-fit-one association) in Qian et al. (2021) to the above inequality, and for some constant $\lambda \geq 3$ we have

$$\max_{c_i,c_j\in\mathcal{S}_s^*,i\neq j}\|c_j-c_i\|_2 \leq 2\max_{c_i\in\mathcal{S}_s^*}\|c_i-\theta_s^*\|_2 \leq 16\lambda k^2\sqrt{r\Delta_{max}}. \tag{39}$$

By combining the above inequality and the assumption $\Delta_{min} \geq 10\eta\lambda k^2\sqrt{r\Delta_{max}}$ in (36), we obtain

$$\max_{c_i,c_j\in\mathcal{S}_s^*,i\neq j}\|c_j-c_i\|_2 \leq \frac{8}{5\eta}\Delta_{min}, \tag{40}$$

where the constant $\eta \geq 5$. Next, we derive the approximation error between $\tilde{\Delta}_{min}^{(m)}$ and Δ_{min} as:

$$\begin{aligned}|\tilde{\Delta}_{min}^{(m)}-\Delta_{min}| &\leq \max_{c_s\in\mathcal{S}_s^*}\|c_s-\theta_s^*\|_2+\max_{c_{s'}\in\mathcal{S}_{s'}^*}\|c_{s'}-\theta_{s'}^*\|_2, \qquad s\in[k], s'\in[k], s\neq s'\\ &\leq\ 2\max_{c_s\in\mathcal{S}_s^*}\|c_s-\theta_s^*\|_2, \qquad s\in[k]. \end{aligned}\tag{41}$$

Given that all clients follow the same mixture distributions under the Stochastic Ball Model, the above inequality holds for all clients $m \in [M]$. Similar to inequality (38), we again utilize the error bound from Theorem 1 (many/one-fit-one association) in Qian et al. (2021), and obtain:

$$|\tilde{\Delta}_{min}^{(m)}-\Delta_{min}| \leq \frac{8}{5\eta}\Delta_{min}, \qquad \forall m\in[M]. \tag{42}$$

Reorganizing the terms in inequality (42) gives

$$\frac{5\eta}{5\eta+8}\tilde{\Delta}_{min}^{(m)} \leq \Delta_{min} \leq \frac{5\eta}{5\eta-8}\tilde{\Delta}_{min}^{(m)}, \qquad \forall m\in[M]. \tag{43}$$

Then by combining inequalities (40) and (43), for each $s \in [k]$, we obtain

$$\max_{c_i,c_j\in\mathcal{S}_s^*,i\neq j}\|c_j-c_i\|_2 \leq \frac{8}{5\eta-8}\tilde{\Delta}_{min}^{(m)} \leq \frac{1}{2}\tilde{\Delta}_{min}^{(m)}, \qquad \forall m\in[M], \tag{44}$$

where the last inequality follows from the assumption that $\eta \geq 5$. □

A.3 Proof of Theorem 4.1

In this section, we complete the proof of our main theorem by demonstrating: (1) Algorithm 5 correctly classifies all returned centroids in alignment with their corresponding true centers, utilizing the radius assigned by Algorithm 3; (2) we derive the error bound between the final output centroids $\mathcal{C}^*$ from our main Algorithm 1 and the true centers.

Proof. Let cluster labels be $s = 1, \ldots, k$. During the grouping process of all returned centroids $\mathcal{C}$ on the server end, Algorithm 5 first selects a centroid in $\mathcal{C}$ accompanying with the largest radius. Without loss of generality, we assume that this selected centroid $c_s \in \mathcal{C}$ associates with the true center θ_s^*, and is returned by the client m. Thus, this centroid belongs to the ground truth clustering set as $c_s \in \mathcal{S}_s^*$ and its assigned radius is $r_s = \frac{1}{2}\tilde{\Delta}_{min}^{(m)}$. Algorithm 5 then groups the centroids located within the area centered at c_s and bounded by the radius r_s, resulting in the formation of the grouped cluster $\mathcal{S}_s = \{c : c \in \mathcal{C}, \|c - c_s\| \leq r_s\}$.

On the one hand, Lemma A.3 implies that for each $s \in [k]$, the maximum pairwise distance between centroids in $\mathcal{S}_s^*$ is bounded by $\frac{1}{2}\tilde{\Delta}_{min}^{(m)}$ for any client m. Consequently, $\mathcal{S}_s^* \in \mathcal{S}_s$ can be readily inferred based on the definition of $\mathcal{S}_s$.

On the other hand, for other centroids $c_{s'} \in \mathcal{S}_{s'}^*, s' \in [k], s \neq s'$, we have

$$\begin{aligned} \|c_{s'} - c_s\|_2 &\geq \|\theta_{s'}^* - \theta_s^*\|_2 - \|c_{s'} - \theta_{s'}^*\|_2 - \|c_s - \theta_s^*\|_2 \\ &\geq \Delta_{min} - \|c_{s'} - \theta_{s'}^*\|_2 - \|c_s - \theta_s^*\|_2. \end{aligned} \tag{45}$$

Utilizing the error bound from Theorem 1 (many/one-fit-one association) in Qian et al. (2021) gives

$$\|c_{s'} - c_s\|_2 \geq \Delta_{min} - 16\lambda k^2\sqrt{r\Delta_{max}} \geq \Delta_{min} - \frac{8}{5\eta}\Delta_{min}, \tag{46}$$

where the last step follows from the assumption $\Delta_{min} \geq 10\eta\lambda k^2\sqrt{r\Delta_{max}}$. Applying the lower bound in (43) to the above inequality, for any client $m \in [M]$, it follows that

$$\|c_{s'} - c_s\|_2 \geq \frac{5\eta - 8}{5\eta + 8}\tilde{\Delta}_{min}^{(m)} > \frac{1}{2}\tilde{\Delta}_{min}^{(m)}, \tag{47}$$

where the constant $\eta \geq 5$. Thus, following the definition of $\mathcal{S}_s$, the above inequality implies that centroids $c_{s'} \in \mathcal{S}_{s'}^*, s \neq s'$ do not belong to $\mathcal{S}_s$. Combining the proved claim that $\mathcal{S}_s^* \in \mathcal{S}_s$, this suggests that $\mathcal{S}_s = \mathcal{S}_s^*, s \in [k]$, up to permutation of cluster labels. This further implies that Algorithm 5 correctly classifies all returned centroids in $\mathcal{C}$ according to their associated true centers.

For each $s \in [k]$, Algorithm 5 computes the mean of $\mathcal{S}_s$, denoted as $c_s^* = \text{mean}(\mathcal{S}_s)$. The collection of these mean centroids, $\mathcal{C}^* = \{c_1^*, \ldots, c_k^*\}$, constitutes the final set of centroids output by Algorithm 1. The proximity of c_s^* to its corresponding true center θ_s^* can be bounded as:

$$\|c_s^* - \theta_s^*\|_2 \leq \max_{c \in \mathcal{S}_s} \|c - \theta_s^*\|_2 \leq \max_{c \in \mathcal{S}_s^*} \|c - \theta_s^*\|_2, \quad \forall s \in [k] \tag{48}$$

$$\leq 8\lambda k^2\sqrt{r\Delta_{max}} \leq \frac{4}{5\eta}\Delta_{min}, \tag{49}$$

for some constants $\eta \geq 5$. The inequality (48) follows from the proved statement $\mathcal{S}_s = \mathcal{S}_s^*$, $s \in [k]$. The inequality (49) first utilizes the error bound from Theorem 1 (many/one-fit-one association) in Qian et al. (2021), followed by the application of the separation assumption $\Delta_{min} \geq 10\eta\lambda k^2\sqrt{r\Delta_{max}}$.

□

B Evaluation on the radius assigned by Algorithm 4 (*Empirical*).

This section evaluates the radius produced by the empirical algorithm variant, Algorithm 4. While the proof of our main theorem characterizes the performance of the theoretical algorithm variant, it is important to note that most real-world scenarios do not adhere to a homogeneous data split assumption. Consequently, we have implemented an empirical algorithm that assigns a unique radius to each returned centroid. In this context, it is also not necessary to remove many-fit-one centroids on clients, as these centroids typically concentrate around true centers and will be grouped together via the aggregation algorithm on the server. This empirical algorithm variant is specifically designed to adapt our main algorithm FeCA for more practical scenarios.

In this analysis, we empirically assess the radius assigned by Algorithm 4 under both IID and non-IID scenarios, demonstrating its effectiveness in guiding the aggregation step in Algorithm 5. Specifically, our objective is to empirically show that utilizing the selected centroid-radius pair $(c_s, r_s), s \in [k]$ (assigned by Algorithm 4), Algorithm 5 can effectively group all returned centroids that are corresponding to the same true center θ_s^* on the server end. Recall that we denote a set of returned centroids associated with one true center θ_s^* as $\mathcal{S}_s^*$.

Essentially, we aim to validate that the distance between any centroid $c \in \mathcal{S}_s^*$ to c_s is bounded by the radius r_s. Our goal is thus formulated as follows:

$$\max_{c_i \in \mathcal{S}_s^*} \|c_i - c_s\|_2 \leq r_s. \tag{50}$$

The left side of the above inequality indicates the maximum distance between any two centroids in $\mathcal{S}_s^*$, and it can be further elaborated as

$$\max_{c_i \in \mathcal{S}_s^*} \|c_i - c_s\|_2 \leq \max_{c_s \in \mathcal{S}_s^*} (\|c_i - \theta_s^*\|_2 + \|\theta_s^* - c_s\|_2) \leq 2 \max_{c_i \in \mathcal{S}_s^*} \|c_i - \theta_s^*\|_2. \tag{51}$$

Then our goal in (50) can be reformulated as

$$\max_{c_i \in \mathcal{S}_s^*} \frac{\|c_i - \theta_s^*\|_2}{r_s} \leq \frac{1}{2}. \tag{52}$$

Next, we present empirical results on the synthetic dataset, S-sets (S1), with known ground truth centers $\{\theta_s^*\}_{s \in [k]}$. These results demonstrate that the inequality (52) holds across both IID and non-IID cases. For

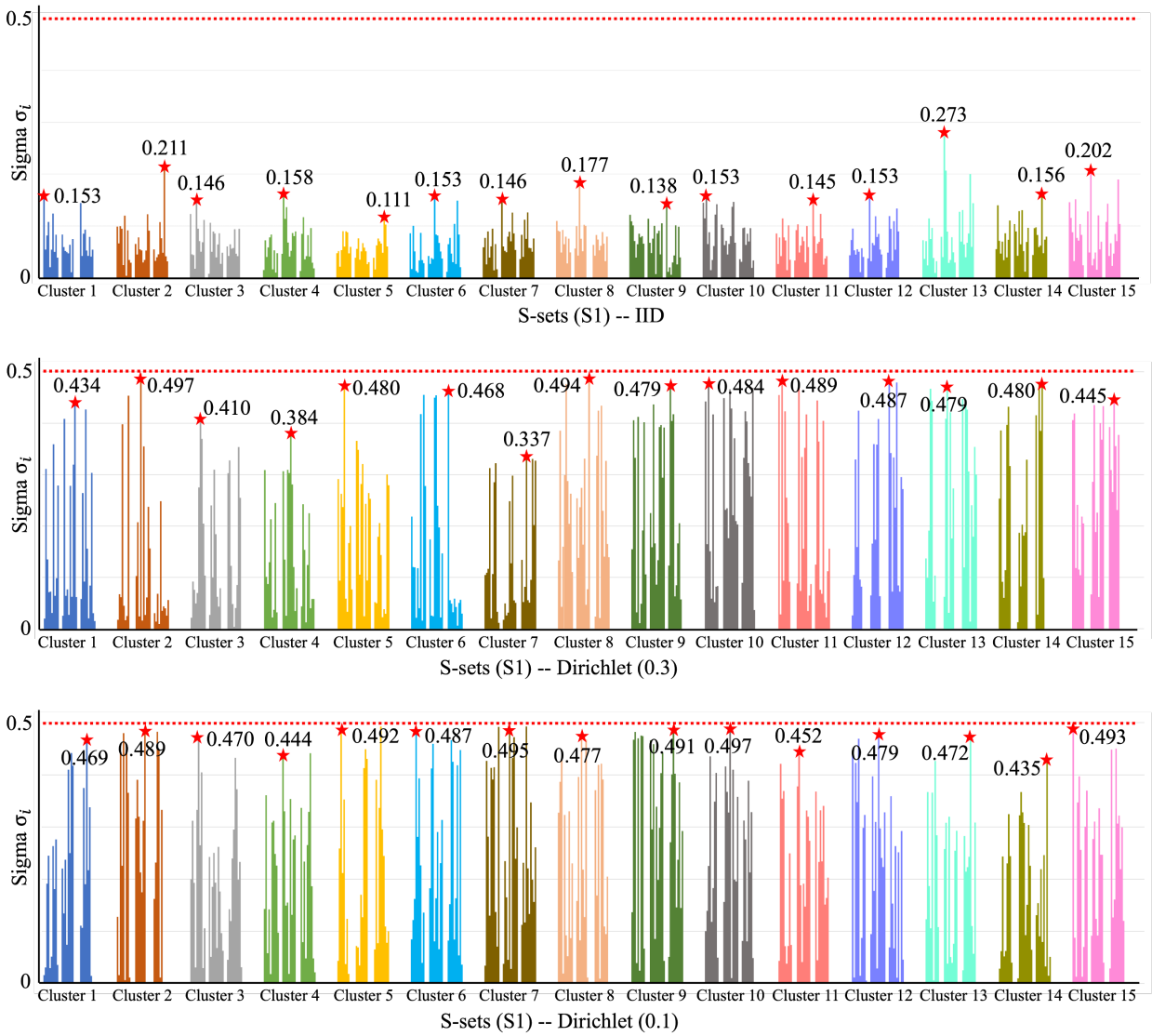

Figure 5: **Evaluation of σ on S-sets (S1) across three data split conditions.** σ_i for k clusters is represented in different colors. The values of σ_i for all returned centroids c_i are reported over 3 random runs, with the red star marking the maximum σ_i observed in three runs. *A σ_i value below* 0.5 *indicates that, the server effectively groups centroid c_i utilizing the radius r_s assigned by Algorithm 4.*

this purpose, we define a new parameter σ as

$$\sigma_i := \frac{\|c_i - \theta_s^*\|_2}{r_s}, \quad c_i \in \mathcal{S}_s^* \quad s \in [k]. \tag{53}$$

This parameter σ_i represents the distance between the returned centroid c_i and its fitted true center θ_s^* scaled by the radius r_s. Our empirical results demonstrate that values of σ_i remain below 0.5 for all returned centroids in $\mathcal{C} = \{\mathcal{C}^{(1)}, \ldots, \mathcal{C}^{(M)}\}$, in accordance with our goal inequality (52).

Results. Figure 5 illustrates the evaluation of σ_i, as determined using the radius assigned by Algorithm 4, in varied inhomogeneous settings on S-sets (S1). This figure presents σ_i values for all returned centroids across three random runs, categorized according to their respective true centers in different colors. Result consistently indicate that σ_i values stay below 0.5, thereby empirically substantiating the validity of the inequality (52) in our analysis. Consequently, it demonstrates the efficacy of aggregating centroids using the radius assigned by Algorithm 4 on the server end.

We note that the number of returned centroids associated with each true center may vary. It is because we selectively remove one-fit-many centroids on the client side, while it is possible for many-fit-one centroids to be present. In some extreme non-IID cases, assuming a client only contains a few secluded data points from one true cluster but they all far deviate from the true center, it may occur that a returned centroid is not covered by the radius. Then it will be considered noisy and discarded by Algorithm 5. Concretely, the recovered centroids of this cluster will be contributed by returned centroids from other clients.

C Supplementary experiments on the synthetic dataset

This section presents additional experimental results on the synthetic dataset S-sets Fränti & Sieranoja (2018). The S-sets comprise four sets: S1, S2, S3, and S4, each consisting of 15 Gaussian clusters in 2-dimensional data with varying degrees of overlap, specifically $9\%, 22\%, 41\%$, and 44%. For the visualization of S-sets, refer to Figure 6 from their paper Fränti & Sieranoja (2018).

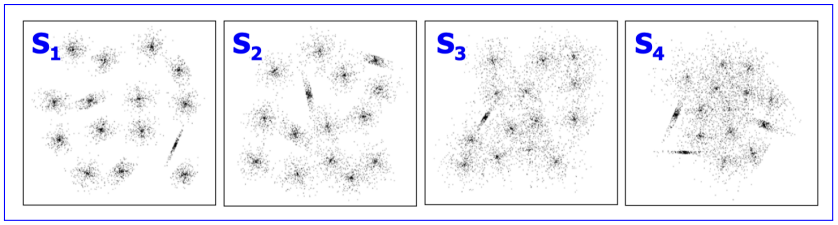

Figure 6: **Visualizations of S-sets.**

C.1 ~~Standard deviation of ℓ_2-distance results in~~

~~This section presents additional experimental findings that complement the results outlined in . We report the standard deviation of the ℓ_2-distance measurements, scaled by a factor of 10^4, across 10 random runs, as summarized in . Additionally, we provide illustrations of the ℓ_2-distance outcomes, utilizing 10 random seeds for S-sets(S2) and S-sets(S3), as depicted in .~~

~~These supplementary experimental results underscore the efficacy and stability of our proposed algorithm, , in accurately approximating the ground truth centers when compared against all baseline methods across diverse federated data split scenarios. This analysis not only highlights the reliability of but also showcases its superior performance in handling heterogeneous federated learning environments.~~

~~**The standard deviation (scaled by 10^4) of ℓ_2-distance detailed in . Standard Deviation**~~

~~Method IID (0.3) (0.1) IID (0.3) (0.1) IID (0.3) (0.1) IID (0.3) (0.1) M-Avg 4.3 5.0 2.8 7.1 8.9 11.1 6.8 5.7 5.3 3.7 3.3 6.4~~

~~FFCMv1(Rd=1) 15.8 13.3 15.7 20.4 13.3 16.0 15.2 11.9 8.9 9.5 8.9 10.8~~

~~FFCMv1(Rd=10) 1.4 8.8 12.4 19.1 12.3 18.2 15.5 8.8 12.9 1.3 12.3 11.9~~

~~FFCMv2(Rd=1) 19.4 16.8 14.4 16.9 13.5 12.6 12.6 12.6 10.2 11.4 9.7 9.6~~

~~FFCMv2(Rd=10) 0.4 14.8 14.6 0.5 13.5 25.8 0.7 19.3 16.7 0.6 9.1 7.3~~

~~k-FED(k'=5) 15.8 12.3 16.9 17.7 13.1 11.6 14.3 15.2 12.8 10.8 6.3 8.6~~

~~0.1 3.7 15.6 0.1 16.1 3.4 0.7 8.8 6.7 0.7 7.2 5.8Centralized~~

~~**Illustrations of ℓ_2-distance results in for S-sets(S2&S3) using 10 random seeds.**~~

C.1 ~~More visualizations on the synthetic dataset~~

~~To better understand the local solution structures as discussed in , we demonstrate some local solutions of centralized k-means on the synthetic dataset S-sets, shown in . This visualization reveals that despite different degrees of separations between the ground truth centers, Lloyd's algorithm often encounters suboptimal solutions containing both one-fit-many and many-fit-one centroids. This leads to poor performance and highlights the necessity of resolving such local solutions to improve stability and accuracy.~~

~~**Visualizations of local solutions of centralized k-means on S-sets.**~~

~~To further demonstrate the superior performance of our algorithm, we present more visualizations corresponding to the results detailed in for S-sets(S2) and S-sets(S3). displays the centroids recovered by various federated clustering algorithms under the non-IID condition – Dirichlet(0.3). Our algorithm's ability to resolve and leverage the structures of local solutions enables it to outperform other baseline methods that fail to address these critical aspects, especially in challenging non-IID settings. This emphasizes the critical role of resolving and utilizing local solutions for enhanced algorithmic performance.~~

~~**Visualizations of S-sets (S2&S3) and recovered centroids by different methods.** Results are showcased under the Dirichlet(0.3) data split condition. Blue dots represent recovered centroids, and red crosses indicate the ground truth centers.~~

C.1 Evaluations on the clustering assignments

This section shifts focus to the evaluation of clustering assignments on the synthetic dataset S-sets, diverging from the analysis of recovered centroids. While Table 1 in the paper assesses the ℓ_2 distance between recovered centroids and known ground truth centers, we herein present the average results of Purity and NMI across 10 random runs in Table 4 under three different data split strategies. The findings consistently demonstrate that our algorithm FeCA surpasses all baseline algorithms in performance across every tested scenario, underlining its effectiveness in federated clustering tasks.

C.2 More visualizations of recovered centroids by different methods on S-sets

To further demonstrate the superior performance of our algorithm, we present more visualizations corresponding to the results detailed in Table 1 for S-sets(S2) and S-sets(S3). Figure 7 displays the centroids recovered by various federated clustering algorithms under the non-IID condition – Dirichlet(0.3). Our algorithm's ability to resolve and leverage the structures of local solutions enables it to outperform other baseline methods that fail to address these critical aspects, especially in challenging non-IID settings. This emphasizes the critical role of resolving and utilizing local solutions for enhanced algorithmic performance.

C.3 Ablation study on eliminating one-fit-many centroids in Algorithm 2

Removing one-fit-many centroids in Algorithm 2 plays a crucial role in enhancing the algorithm's performance. These centroids are typically far from any true centers. By eliminating one-fit-many centroids at the client end, we effectively prevent the transmission of these problematic centroids to the server. It

Table 4: **Purity and NMI on S-sets under three data split conditions.**

Purity	S-sets (S1)			S-sets (S2)			S-sets (S3)			S-sets (S4)		
Method	IID	(0.3)	(0.1)	IID	(0.3)	(0.1)	IID	(0.3)	(0.1)	IID	(0.3)	(0.1)
M-Avg	0.99	0.79	0.69	0.93	0.74	0.68	0.80	0.66	0.61	0.75	0.64	0.57
FFCMv1 (Rd=1)	0.97	0.69	0.66	0.95	0.68	0.58	0.83	0.60	0.54	0.79	0.60	0.53
FFCMv1 (Rd=10)	0.98	0.78	0.68	0.96	0.74	0.71	0.85	0.66	0.57	0.80	0.61	0.55
FFCMv2 (Rd=1)	0.95	0.69	0.66	0.95	0.63	0.61	0.83	0.58	0.52	0.78	0.57	0.54
FFCMv2 (Rd=10)	0.99	0.80	0.76	0.97	0.70	0.72	0.86	0.65	0.61	0.80	0.60	0.59
k-FED (k'=5)	0.62	0.76	0.75	0.60	0.71	0.71	0.55	0.61	0.60	0.55	0.62	0.58
FeCA	**0.99**	**0.98**	**0.96**	**0.97**	**0.95**	**0.90**	**0.86**	**0.80**	**0.78**	**0.80**	**0.73**	**0.65**
Centralized		0.97			0.96			0.83			0.77	

NMI	S-sets (S1)			S-sets (S2)			S-sets (S3)			S-sets (S4)		
Method	IID	(0.3)	(0.1)	IID	(0.3)	(0.1)	IID	(0.3)	(0.1)	IID	(0.3)	(0.1)
M-Avg	0.98	0.85	0.79	0.92	0.80	0.78	0.77	0.71	0.69	0.70	0.65	0.62
FFCMv1 (Rd=1)	0.98	0.80	0.78	0.93	0.77	0.71	0.78	0.67	0.64	0.72	0.63	0.60
FFCMv1 (Rd=10)	0.98	0.85	0.80	0.94	0.80	0.78	0.79	0.71	0.66	0.72	0.64	0.61
FFCMv2 (Rd=1)	0.97	0.80	0.78	0.93	0.75	0.72	0.78	0.67	0.63	0.71	0.62	0.60
FFCMv2 (Rd=10)	0.99	0.87	0.85	0.95	0.78	0.79	0.79	0.70	0.68	0.72	0.63	0.63
k-FED (k'=5)	0.80	0.84	0.83	0.75	0.80	0.80	0.66	0.69	0.68	0.62	0.65	0.63
FeCA	**0.99**	**0.96**	**0.95**	**0.95**	**0.94**	**0.90**	**0.80**	**0.77**	**0.75**	**0.72**	**0.69**	**0.66**
Centralized		0.98			0.94			0.79			0.71	

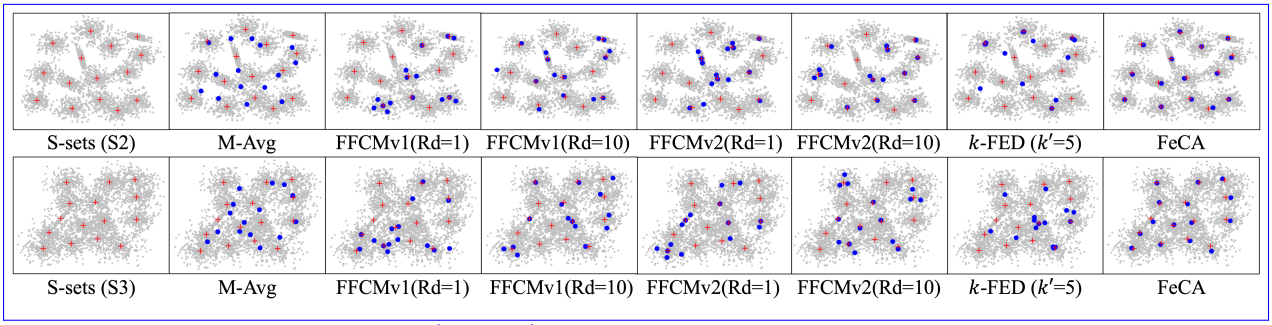

Figure 7: **Visualizations of S-sets (S2&S3) and recovered centroids by different methods.** Results are showcased under the Dirichlet(0.3) data split condition. Blue dots represent recovered centroids, and red crosses indicate the ground truth centers.

significantly simplifies the task of Algorithm 5 on the server side, which involves grouping received centroids close to the same true center.

In this section, we conduct an ablation study on eliminating one-fit-many centroids in Algorithm 2. In the following experiments, one-fit-many centroids are not removed on clients and then sent to the server. We present mean square errors between recovered centroids and ground truth centers in Table 5. The comparative results clearly demonstrate a performance degradation when these centroids are not removed, underscoring the significance of eliminating the one-fit-many step in Algorithm 2.

Table 5: **Mean square errors between recovered centroids and true centers on S-sets(S1) under IID data split condition.** Values of MSE are scaled by 10^6. We report mean results from 10 random runs.

Method	MSE $\times 10^6$
FeCA(not removing one-fit-many centroids)	12977.2
FeCA(removing one-fit-many centroids)	**6.7**

Not enough output centroids. Not removing one-fit-many centroids can lead to a scenario where the number of reconstructed centroids is less than k. This occurs because the cluster of one-fit-many centroids typically contains data points from multiple true clusters, resulting in a significantly larger radius than that assigned to the true cluster. Consequently, the server may prioritize these centroids with large radii during the grouping process, forming a large group erroneously containing centroids associated with different true centers. In Figure 8, we provide visualizations of reconstructed centroids without removing one-fit-many, demonstrating a notable decrease in performance. This emphasizes the necessity of their removal in our algorithm.

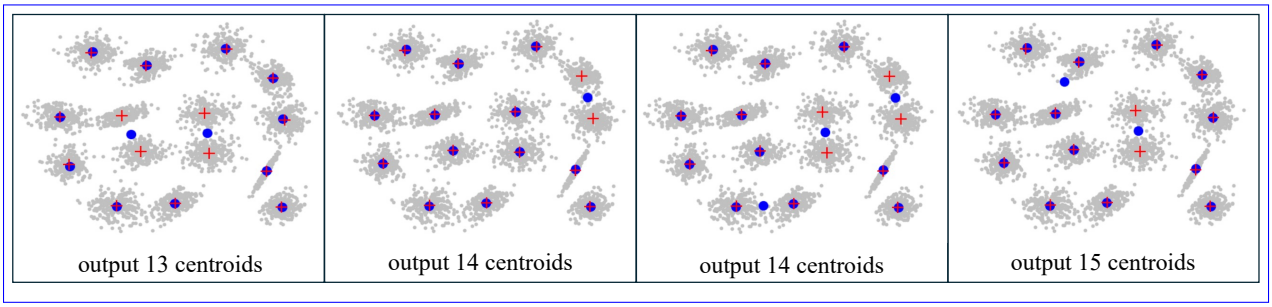

Figure 8: **Visualizations of recovered centroids by FeCA(not removing one-fit-many).** Results are showcased under the IID condition on S-sets(S1). Blue dots represent recovered centroids, and red crosses indicate the ground truth centers.

C.4 Comparison between Algorithm 3 (theoretical) and Algorithm 4 (empirical)

Algorithm 3 (theoretical) is designed for theoretical analysis only under a strict setup, specifically the stochastic ball model assumption. This assumption allows for the straightforward identification and removal of many-fit-one centroids. However, in practical scenarios, eliminating many-fit-ones is challenging and unnecessary, as they often carry crucial information about the global solution.

In this section, we explore the applicability of Algorithm 3 (theoretical) beyond its constraints by conducting experiments on S-sets under various heterogeneous conditions. Table 6 presents results, revealing that the performance of Algorithm 3 is suboptimal when assumptions of stochastic ball model are not met, particularly in non-IID cases. This is due to its reliance on assumptions for identifying many-fit-one centroids. Consequently, in practical scenarios, this approach may erroneously eliminate true centroids, leading to suboptimal outcomes.

Table 6: **ℓ_2-distance (mean±std) between recovered centroids and true centers on S-sets(S1) under different data split conditions.** Values of ℓ_2-distance are scaled by 10^4.

Method	IID	(0.3)	(0.1)
FeCA (theoretical)	1.1 ±0.1	31.8 ± 23.8	58.9 ± 15.1
FeCA (empirical)	**1.0**±0.1	**6.8**±3.7	**22.3**±15.6

C.5 Tuning k' for k-FED on the synthetic dataset

In this section, we provide the results of experiments conducted to select k' for k-FED Dennis et al. (2021) on the synthetic dataset. Given that all four subsets of S-sets have the same number of true clusters $k^* = 15$, here we utilize S-sets(S1), which has the largest degree of separation, for tuning k'. This choice is based on the separation condition mentioned in their paper. We present the ℓ_2-distance between the recovered centroids and true centers for k' values ranging from 2 to 15. And results (mean±std) from 10 random seeds are reported in the Table 7. Additionally, we evaluate the clustering assignments generated from the recovered centroids using Purity and NMI metrics. The mean results from 10 random runs are included in Table 7.

Considering k-FED is designed for heterogeneous scenarios, we adopt a Dirichlet(0.3) non-IID federated data split set in the following experiments. It is also important to note that when $k' = k^*$, the aggregation step in the k-FED algorithm essentially becomes redundant, and the recovered centroids are equivalent to the set of centroids returned by one randomly chosen client.

Table 7: **ℓ_2-distance (mean±std) between recovered centroids and true centers, Purity, and NMI on S-sets(S1) under Dirichlet(0.3) data split condition.** Values of ℓ_2-distance are scaled by 10^4.

k-FED	$k' = 2$	$k' = 3$	$k' = 4$	$k' = 5$	$k' = 6$	$k' = 7$	$k' = 8$
ℓ_2-distance	63.3±7.0	65.9±11.9	60.8±16.8	**58.1±10.7**	60.3±15.0	59.4±11.1	62.5±11.0
Purity	0.71	0.72	0.79	**0.79**	0.78	0.79	0.76
NMI	0.83	0.83	**0.89**	0.88	0.87	0.88	0.87
k-FED	$k' = 9$	$k' = 10$	$k' = 11$	$k' = 12$	$k' = 13$	$k' = 14$	$k' = 15$
ℓ_2-distance	77.3±11.2	69.4±13.8	77.7±15.2	76.4±10.7	72.1±16.1	69.8±15.7	67.4±9.5
Purity	0.72	0.74	0.71	0.72	0.74	0.75	0.78
NMI	0.83	0.84	0.83	0.85	0.85	0.86	0.85

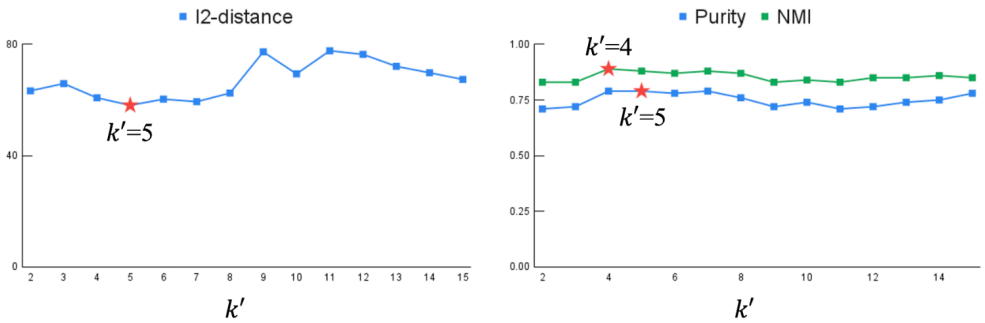

Figure 9: **Illustrations of ℓ_2-distance means, Purity and NMI detailed in Table 7.**

C.6 Presence of local solutions in k-means

In this section, we perform centralized k-means on 50%, 75%, and 100% of data from S-sets. In Figure 10, we illustrate objective values calculated as Equation 1 using 10 random seeds. As depicted, Lloyd's algorithm frequently converges to local solutions with objective values significantly larger than that of global solutions. This empirical result demonstrates the presence of local solutions with poor performance is independent of the data sample size. Thus, it highlights the necessity of our algorithm, which is specifically designed to address and resolve these suboptimal local solutions.

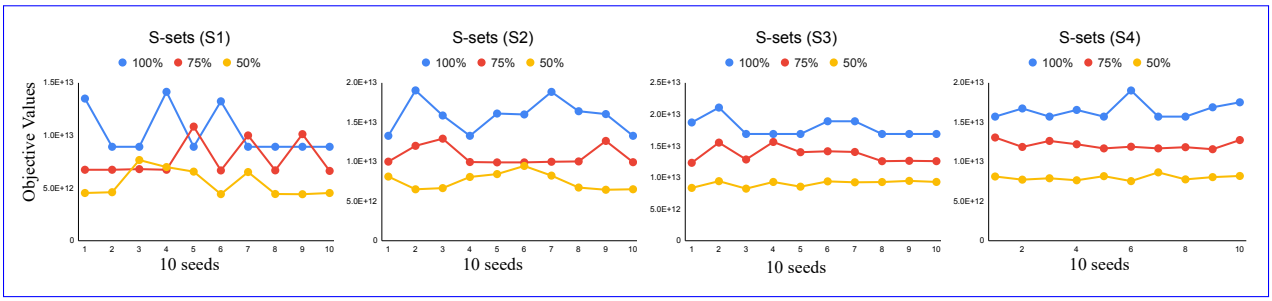

Figure 10: **Objective values of centralized k-neans using 100%, 75%, and 50% of data from S-sets.**

To better understand the structures of local solutions, we visualize some local solutions of centralized k-means on S-sets, shown in Figure 11. This visualization reveals that despite variations in data separations,

spurious local solutions exhibit structures as discussed in subsection 3.1, containing both one-fit-many and many-fit-one centroids. This emphasizes the necessity of the steps in our algorithm that discard one-fit-many and aggregate many-fit-one centroids.

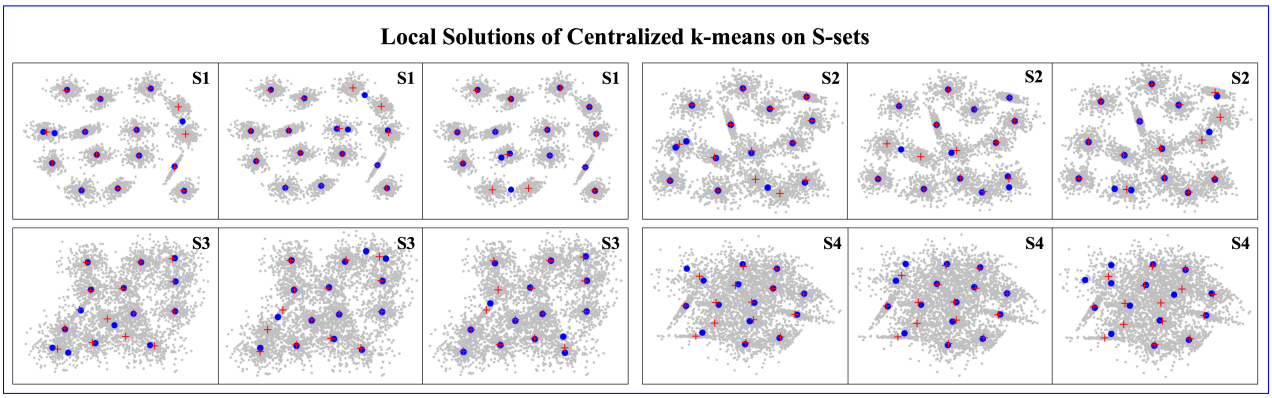

Figure 11: **Visualizations of structured local solutions of centralized k-means on S-sets.**

Almost-empty cases. As outlined in Qian et al. (2021), local solutions of k-means can be composed of one/many-fit-one, one-fit-many and almost-empty centroids. The first two have been discussed in detail in subsection 3.1. Addressing almost-empty cases involves identifying centroids that are far from any true centers and its cluster is almost empty with a small measure. This typically occurs when the dataset contains isolated points that are significantly far from the true centers. It is worth noting that almost-empty cases are more theoretical than practical, with rare occurrences in empirical experiments.

However, if such a case does occur, our algorithm can handle it in the aggregation step (Algorithm 5). Centroids from almost-empty clusters can be treated as noisy data and discarded during the grouping process. Since they are distant from true centers and other received centroids, they do not contribute meaningfully to the final grouping.

D Discussion on varying numbers of clients

In this section, we explore the impact of varying client numbers on our federated approach. We conduct experiments by allocating a fixed dataset portion (5% randomly sampled from the entire dataset) to each client and then perform our algorithm FeCA across varying numbers of clients. We first evaluate the recovered centroids by calculating ℓ_2-distance between these centroids and the ground truth centers. Subsequently, we apply a one-step Lloyd's algorithm using the recovered centroids for initialization and then evaluate the clustering assignments by calculating Purity and NMI. Results for the S-sets (S1) are presented in Table 8. It is noteworthy that only centralized k-means clustering is performed when the number of clients is one. In such cases, centralized k-means often results in large ℓ_2-distance due to convergence to local optima with suboptimal performance.

The findings presented in Table 8 are visually depicted in Figure 12 (left), where a trend of decreasing ℓ_2-distance is observed as the number of clients M increases. This trend indicates that collaboration among multiple clients can significantly mitigate the negative impact of local solutions. Specifically, when a client encounters a local minimum, integrating benign results from other clients can help alleviate this issue. This collaborative mechanism underscores the effectiveness of federated approaches in improving performance by leveraging the distributed nature of client contributions.

Additionally, we assess the impact of varying client numbers in a standard federated setting, particularly under IID data split condition for S-sets(S1). In the following experiments, with M denoting the number of clients, each client is allocated $\frac{1}{M}$ of the data points from S-sets(S1). We note that centralized k-means is performed when $M = 1$ on the entire dataset. We evaluate the performance of our algorithm FeCA by

Table 8: **ℓ_2-distance (mean±std) between recovered centroids and true centers, Purity, and NMI with different numbers of clients M.** Values of ℓ_2-distance are scaled by 10^4. Each client possesses 5% data of S-sets(S1).

FeCA	$M=1$	$M=2$	$M=3$	$M=4$	$M=5$	$M=6$	$M=7$	$M=8$	$M=9$	$M=10$
ℓ_2-distance	10.7±14.3	3.1±0.6	2.6±0.4	2.1±0.3	2.0±0.3	1.7±0.3	1.8±0.2	1.6±0.4	1.4±0.2	1.4±0.3
Purity	0.98	0.99	0.99	0.99	0.99	0.99	0.99	0.99	0.99	0.99
NMI	0.98	0.99	0.99	0.99	0.99	0.99	0.99	0.99	0.99	0.99
FeCA	$M=11$	$M=12$	$M=13$	$M=14$	$M=15$	$M=16$	$M=17$	$M=18$	$M=19$	$M=20$
ℓ_2-distance	1.3±0.2	1.4±0.3	1.3±0.2	1.4±0.2	1.2±0.2	1.2±0.1	1.1±0.1	1.1±0.1	1.0±0.1	1.0±0.1
Purity	0.99	0.99	0.99	0.99	0.99	0.99	0.99	0.99	0.99	0.99
NMI	0.99	0.99	0.99	0.99	0.99	0.99	0.99	0.99	0.99	0.99

reporting the ℓ_2-distance between recovered centroids and true centers, alongside the Purity and NMI of clustering assignments, detailed in Table 9. Moreover, Figure 12 (right) features visual representations of the ℓ_2 distance results, emphasizing the robustness of our federated algorithm FeCA across varying numbers of clients.

Table 9: **ℓ_2-distance (mean±std) between recovered centroids and true centers, Purity, and NMI with different numbers of clients M.** Values of ℓ_2-distance are scaled by 10^4. Each client possesses $\frac{1}{M}$ data of S-sets(S1).

FeCA	$M=1$	$M=2$	$M=3$	$M=4$	$M=5$	$M=6$	$M=7$	$M=8$	$M=9$	$M=10$
ℓ_2-distance	14.3±18.7	1.1±0.3	1.2±0.3	1.1±0.2	1.1±0.2	1.2±0.2	1.1±0.1	1.1±0.1	1.0±0.1	1.0±0.1
Purity	0.97	0.99	0.99	0.99	0.99	0.99	0.99	0.99	0.99	0.99
NMI	0.98	0.99	0.99	0.99	0.99	0.99	0.99	0.99	0.99	0.99
FeCA	$M=11$	$M=12$	$M=13$	$M=14$	$M=15$	$M=16$	$M=17$	$M=18$	$M=19$	$M=20$
ℓ_2-distance	1.1±0.1	1.1±0.1	1.1±0.2	1.1±0.1	1.1±0.1	1.0±0.2	1.1±0.2	1.1±0.1	1.1±0.1	1.1±0.1
Purity	0.99	0.99	0.99	0.99	0.99	0.99	0.99	0.99	0.99	0.99
NMI	0.99	0.99	0.99	0.99	0.99	0.99	0.99	0.99	0.99	0.99

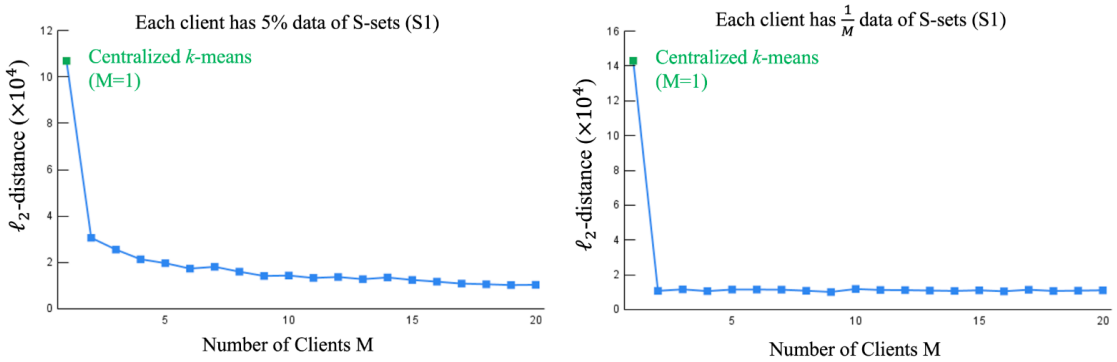

Figure 12: **Illustrations of ℓ_2-distance in Table 8 and Table 9.**

E Discussion on varying k

The selection of k is an important aspect of the k-means problem. In this section, we present supplementary experiments investigating the performance of our algorithm with varying k. For clarity, in this study, we use k to denote the number of recovered centroids desired by our algorithm, which is also the number of output centroids by Algorithm 5. k' denotes the parameter used to perform k-means clustering on clients in Algorithm 2, while k^* indicates the number of true centers. In the following, we present experiments with varying values of k' and k, respectively.

Varying values of k'. We perform FeCAon S-sets(S1) under IID conditions, varying values of k'. We chose $k' = 10$ (undershoot case) and $k' = 20$ (overshoot case) with $k^* = 15$. Mean square errors between recovered centroids and ground truth centers are shown in Table 10. Note that for undershoot cases, the number of recovered centroids k might be less than k^*. In these instances, we identify the top k matching centroids with recovered centroids from k^* true centers and calculate the mean square error between them. Visualizations of clustering results on clients and recovered centroids are illustrated in Figure 13 and Figure 14.

When $k' \neq k^*$, even if clients converge to the global solution, this global solution exhibits similar structures (one-fit-many and many-fit-one) to those observed in local solutions when $k' = k^*$. As shown in Figure 13, when $k' = 10$, clients' clustering results demonstrate the presence of one-fit-many, while $k' = 20$ showcases many-fit-one structures illustrated in Figure 14. Therefore, this underscores the necessity of our algorithm, as it effectively addresses such structured solutions.

Table 10: **Mean square errors between recovered centroids and true centers on S-sets(S1) under IID data split condition.** Values of MSE are scaled by 10^6. We report mean results from 10 random runs.

Methods	k	k'	k^*	MSE $\times 10^6$
FeCA- Varying k' (undershoot case)	15	10	15	34599.4
FeCA- Varying k' (overshoot case)	15	20	15	9.9
FeCA- Varying k	10	15	15	8.4
FeCA	15	15	15	**6.7**

In the undershoot case when $k' = 10$, clients' clustering results might contain multiple one-fit-many but no many-fit-one centroids. This complicates the elimination of one-fit-many centroids in Algorithm 2, because identifying one-fit-many becomes challenging without many-fit-one centroids for reference. As discussed in subsection C.3, if one-fit-many centroids are not eliminated on clients, the number of output centroids k may be less than k^*, shown in Figure 13.

In contrast, in the overshoot case when $k' = 20$, as discussed in subsection 4.2, elimination of many-fit-one centroids on clients is unnecessary, as they can contribute meaningfully to the grouping process on the server end. Therefore, FeCAcan still accurately approximate true centers, as demonstrated in Figure 14.

Varying values of k. We perform FeCAon S-sets(S1) under the IID condition, selecting $k' = k^* = 15$, and $k = 10$. Mean square errors between recovered centroids and ground truth centers are reported in Table 10. When $k < k^*$, Algorithm 5 outputs the mean centroids of the top k groups containing the largest number of elements. As illustrated in Figure 15, even with $k < k^*$, the recovered centroids can still accurately approximate partial true centers.

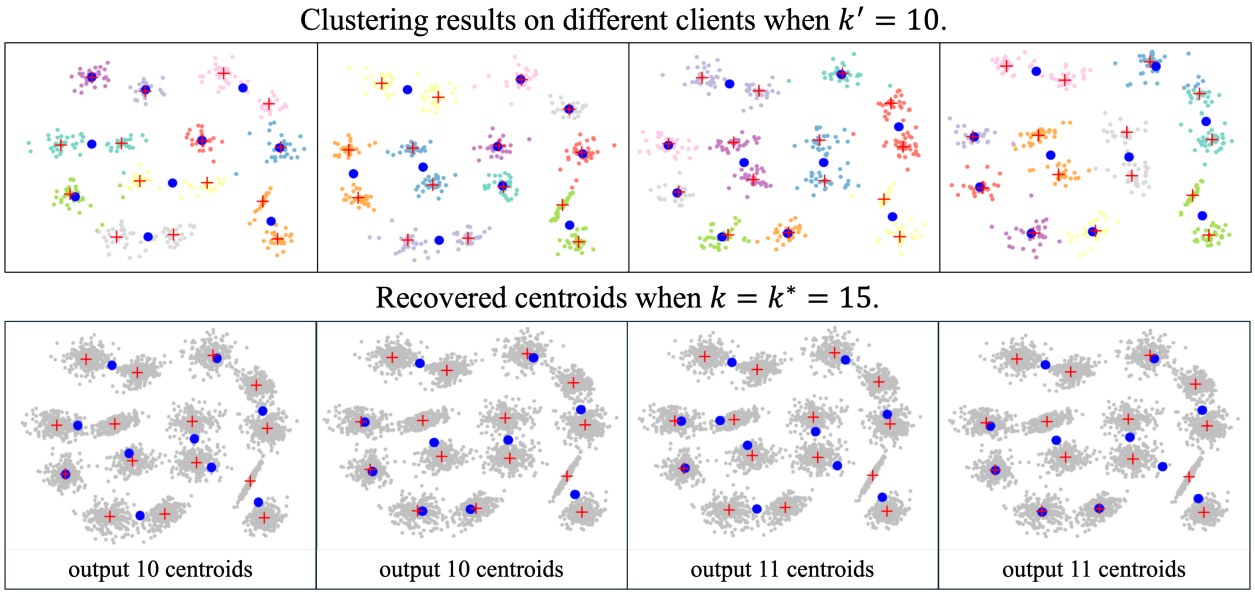

Figure 13: Visualization of clients' clustering results and recovered centroids by **FeCA**.

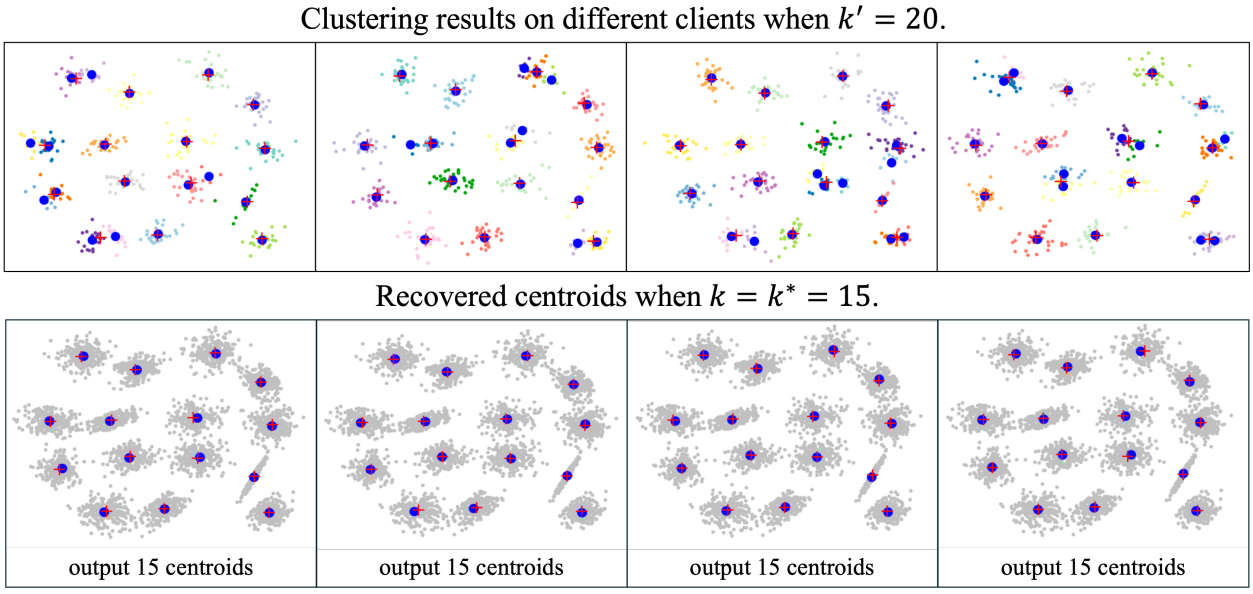

Figure 14: Visualization of clients' clustering results and recovered centroids by **FeCA**.

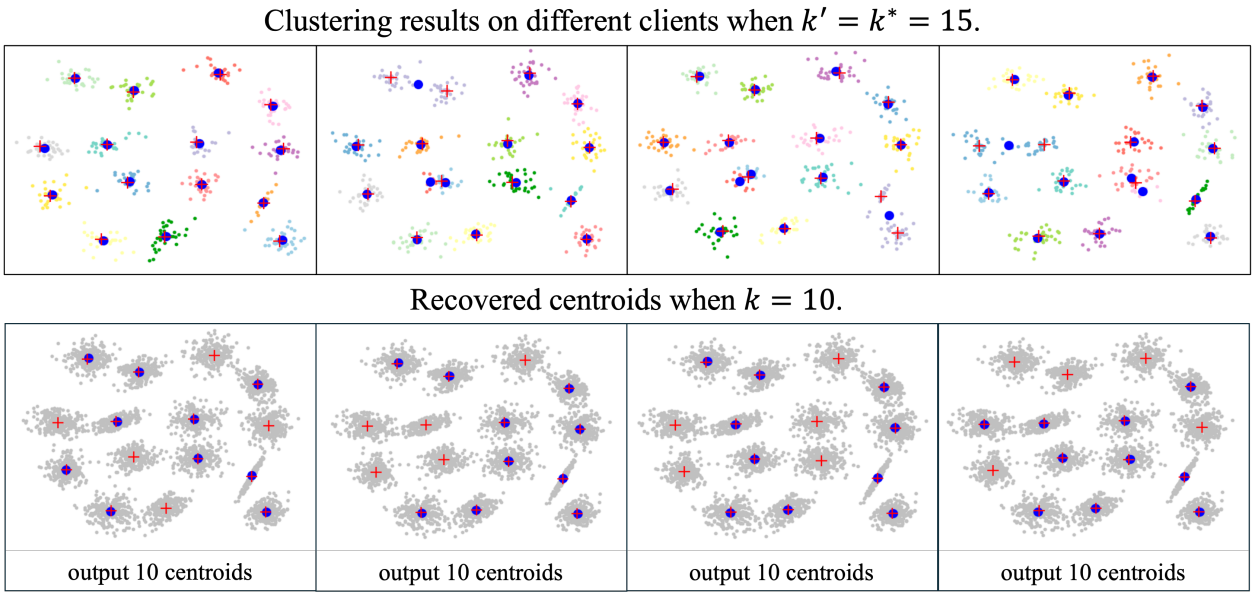

Figure 15: Visualization of clients' clustering results and recovered centroids by **FeCA**.